

USGS External Research Program Final Technical Report
Award #01-HQ-GR-0158

REVISING U.S. MOMENT CATALOG
TO LOWER MAGNITUDES

Bradley B. Woods

URS Group, Inc.
566 El Dorado Street.
Pasadena, CA 91101

email: bradley_woods@urscorp.com
tel: (626) 449-7650 / fax: (626) 449-3536

July 11, 2003

REVISING U.S. MOMENT-CATALOG TO LOWER MAGNITUDES

Bradley B. Woods

URS Group, Inc.
 566 El Dorado Street
 Pasadena, CA 91101
 email: bradley_woods@urscorp.com
 tel: (626) 449-7650 / fax: (626) 449-3536

ABSTRACT

The purpose of this work is to provide improved earthquake magnitude information for revising the NEHRP CEUS catalog (Frankel *et al.*, 1996) which is used to generate probabilistic seismic hazard maps for the central and eastern continental U.S (Frankel, 1995). The CEUS catalog is in terms of m_{bLg} (equivalent to m_b in the eastern U.S.), incorporating other magnitude values -- M_w , m_b , M_L and M_s , all from various sources -- by converting them to m_{bLg} equivalents (Mueller *et al.*, 1997). Further, the relations used to convert the different magnitude types to a universal one are simplified and do not account for empirically observed regional differences. Thus, the catalog makes for a heterogeneous magnitude database. This is shown, for example, by regressing and plotting M_w vs. CEUS m_{bLg} ; the result of which does not correspond to the conversion from M_w to m_{bLg} used to generate the catalog. To provide more consistent magnitudes for this catalog, which in turn will provide a more accurate seismic hazard map for the region, we have developed a variant of the coda magnitude (M_C) measurement, which yields accurate, well-constrained, stable, magnitude estimates using time-domain coda measurements of regional short-period seismograms:

$$M_C = \log_{10}(A_c) + a_0 + a_1 \cdot \log_{10}(\tau) + a_2 \cdot \tau + a_3 \cdot \log_{10}(\Delta),$$

where τ is the coda lapse time (measured from origin time), A_c is the coda amplitude measured in the tail portion of the seismogram, and Δ is epicentral distance. This method, a modified extension of Mayeda's (1993) m_{bLg} (Coda) measurement, was adopted for its ready application to analog data as well as digital, and for its small inter-station variance in magnitude estimates, thereby providing stable measurements. Here the method was applied to the digitally-instrumented (broadband) portion (1988+) of the CEUS catalog. Because of the combination of relatively limited seismicity and low seismic attenuation for this region, we were able to apply this measurement to $m_{bLg} > 3.5$ earthquakes, thereby lowering the magnitude threshold from $M_w = 4$, which was the case for a related study of western U.S. earthquakes (Woods, 2002). As the current CEUS catalog magnitudes are in terms of m_{bLg} , we calibrate M_C to the same. It yields inter-station standard errors ranging between 0.13 and 0.16; final network-averaged coda m_{bLg} estimates, regressed with master event m_{bLg} 's have a standard error of 0.19 -- less than that of the CEUS catalog values. Using this method, coda magnitudes were calculated from regional seismograms for 102 1988+ events from the CEUS catalog, in order to provide a revised, more accurate set of earthquake magnitudes for generating the seismic hazard maps. Although for the purposes of predicting and modeling ground motion, seismic moment (M_0) or its magnitude equivalent, M_w , is the preferred means to quantify earthquake size, as M_0 is a direct physical measure of the long-period earthquake source spectrum, there were not enough events in eastern North America (ENA) for the time window considered (1988+) with moments to calibrate the coda magnitude to M_w . However, to provide a better scaling relationship between m_{bLg} and M_w for ENA, a comprehensive compilation of these magnitude pairs was made for earthquakes in the region, and the data regressed, with the result: $M_w \approx m_{bLg} - 0.36$. This result is consistent with the offset known to exist between short-period magnitude estimates of events in the eastern and western U.S. regions, whereby a given size earthquake occurring in the western U.S. yields a m_b between 0.33 and 0.39 magnitude units less than the same size earthquake in the eastern U.S.

INTRODUCTION

The purpose of this study is to revise, with respect to magnitude, the NEHRP seismicity catalog for the central and eastern United States (CEUS; Mueller *et al.*, 1997). This catalog is used to generate probabilistic seismic hazard maps for the region. In generating the 1997 National Seismic Hazard Maps, Frankel (1995) demonstrated that seismic hazard calculations based quantitatively on seismicity catalog information (location, time, and magnitude) yield results similar to those of elaborate studies by teams of experts that integrate various seismic, geophysical, and geological data (EPRI/SOG, 1986). This simpler methodology also has the advantage of being based on objective, quantifiable criteria, *i. e.* the spatial and temporal distribution of earthquakes and their magnitudes. In order to capitalize on the strength of this method, which is its statistical robustness, it is important to use as accurate and comprehensive an earthquake catalog as possible. Earthquake source-spectrum level, quantified by some magnitude scale, is of primary importance, indicating the need for accurate and compatible magnitudes for all catalog events.

Reliable source quantification for earthquake catalogs is important in synthesizing accurate probabilistic seismic hazard maps using this empirical approach. Seismic moment (M_0) or moment magnitude (M_w) is a particularly useful parameter for quantifying seismic sources, as it is a physical parameter derived from seismic source theory and yields a stable measure of the long-period source spectrum of earthquakes; as such, it provides a more direct and physically based estimate of ground motion than do empirically based magnitude scales, such as m_b , M_L or M_s . M_w then can directly compare source sizes between earthquakes in different geophysical regimes and different geographical regions. Further, seismologically based models for estimating strong ground motion use seismic moment to quantify the size of earthquakes.

For these reasons, there is a strong preference for using M_0 , or its magnitude equivalent M_w (Kanamori, 1977), given by:

$$M_w = \frac{2}{3} \cdot \log(M_0) - 10.7, \quad (1)$$

where M_0 is in dyne-cm, to quantify earthquake magnitudes for seismic hazard calculations. The primary reason that all magnitudes are still being converted to m_b (or m_{bLg}) for the CEUS catalog is because of the link to current and historical magnitude measurement practice in eastern North American and the associated earthquake catalogs for the region. It makes more sense then, for modeling ground motions, to use M_w ; however, in order to remain consistent with values in the CEUS catalog, it is necessary to revise earthquake magnitudes in terms of m_{bLg} . Therefore, applying the coda-magnitude method to obtain independent estimates of m_{bLg} for events in the CEUS catalog, in conjunction with obtaining the most reliable M_w - m_{bLg} scaling relation for converting between the two magnitudes, will provide the most comprehensive set of data for quantifying earthquake source size for events in the central and eastern U.S.

The earthquake catalog used to generate the national seismic hazard maps (Mueller *et al.*, 1997) uses a unified magnitude system by converting various magnitude types into m_{bLg} , a regional measurement tied to teleseismic m_b , for the CEUS catalog; whereas for the western U.S. (WUS) catalog, M_w is the primary magnitude to which all others are converted. These conversions are based on very general relationships among the various magnitude scales, such as local or Richter magnitude (M_L), surface-wave magnitude (M_s), and coda (M_C) or coda duration magnitude (M_D) (see Mueller *et al.* (1997) for details). Thus the catalogs are heterogeneous in nature and the magnitude values themselves are sensitive to the magnitude conversion used.

There are several shortcomings to this procedure and the magnitudes so generated. First, there is often a lot of scatter (large variance) in some of these magnitude relations, which is in itself a source of error in the magnitude conversion. Many of the empirical relationships between m_{bLg} and these other magnitude scales are based on regressions within a confined magnitude range ($3 \leq M \leq 5$ for some magnitude scales) and on older analog-data events for which moment measurements are less accurate than for more recent earthquakes which have been digitally recorded regionally and analyzed using current moment-tensor inversion methods. Direct measurement of seismic moment, on the other hand, gives a more accurate estimate of actual source excitation level.

Second, some of these empirical inter-magnitude relations are based on events with m_b 's between 3-5, whereas larger events are of greater importance in computing seismic hazards. Hence these scaling relationships need to be re-examined, using regression analysis, with a more comprehensive set of events, *i. e.* more larger magnitude ($M > 5$) ones, in order to extrapolate the relationship to larger events; otherwise direct magnitude measurements should be made instead -- such as by coda magnitude (M_C) -- which can be made at all magnitude ranges.

We have found by analysis of empirical scaling relationships between M_w and other magnitude scales, using various data sets, that the magnitude conversion formulae currently used to generate the catalog have certain biases which adversely affect the consequent converted magnitude estimates. In the previous study, dealing with the WUS catalog (Woods, 2002), the relationship between the WUS catalogs M_w 's and those compiled from various sources (94 events, total) diverged greatly from the one-to-one scaling relationship (*i. e.* slope of unity and zero offset) used to generate the catalog, being:

$$M_w(\text{WUS}) = 0.90 \cdot M_w(\text{source studies}) + 0.51 \quad (2)$$

and having a large variance, with a standard error of estimate of 0.29 magnitude units. The source-study M_w 's are based on the modeling and inversion of long-period waveforms, and are considered the most accurate estimates of long-period source spectrum for earthquakes. This difference in slope from unity implies that the WUS catalog underestimates the M_w of larger events and correspondingly overestimates the values of smaller events.

Similarly, analogous results for the CEUS catalog are shown in Figure 1, where m_{bLg} (CEUS) is regressed with M_w . The best-fitting, free-slope scaling relationship (a) is near unity (0.95), with a slope unity being within the error bounds. Fixing the slope to unity (b) then is reasonable, however, it yields an offset of 0.2 between the two magnitude scales; whereas the conversion between the two magnitude scales, used to create the CEUS catalog, has a one-to-one correspondence for $M_w \geq 4$ events with zero offset (Mueller *et al.*, 1997). These events' M_w 's and CEUS catalog m_{bLg} 's are provided in Table 1.

From these results it is clear that direct M_w and m_{bLg} measurements need to be made for instrumented events in the CEUS catalogs in order to establish the accuracy of the present catalog values, and, in all likelihood, to revise them with new, improved magnitude estimates obtained in a consistent fashion, which is the purpose of this work, the steps of which are described below. When this is not possible, applying better inter-magnitude scaling relationships, based on more comprehensive regression analysis of other magnitude data sets (catalogs), to the current NEHRP catalog's raw (non- m_{bLg}) magnitudes is another means to achieve this. For this reason, we re-examine the M_w - m_{bLg} relationship for the region.

Whereas the relation between M_w and m_{bLg} for eastern North America (ENA) is not well established, m_{bLg} is tied directly to teleseismic m_b . We verified this relationship by regressing the

m_{bLg} values of larger ($m_{bLg} \geq 4.3$ ENA earthquakes (taken from EPRI, 1986)), with teleseismic m_b , obtained by averaging ISC and NEIC values for the same events, 19 in all. Figure 2 shows the results; the unconstrained slope (a) is poorly constrained; fixing the slope to unity (Figure b) yields a fit just as good (with respect to the standard error of estimate) and with an offset which, when error bounds are accounted for, is near zero. This one-to-one correspondence between these two magnitude scales will be used later, in the DISCUSSION section, to help establish the inter-regional magnitude scaling relationships between western and eastern U.S. (and extended ENA) earthquakes.

To revise m_{bLg} values in the CEUS catalog in a consistent fashion, we employ a coda-magnitude measurement of regional seismograms, calibrated with respect to m_{bLg} . Although we are working only with digitally-recorded events, we use a method that is applicable to analog data as well, and so we use a time-domain measure readily applicable to either type of data. We also want a method useful for the entire range of magnitudes of interest (3.5-6.5). To directly obtain magnitude estimates for smaller events (generally $M_w < 4.5$), for which long-period waveform information generally is not available because of noise-level considerations, requires a method using information from short-period seismograms -- the bandwidth of a short-period World-Wide Seismic Network instrument (WWSP). To this end we employ a measurement of the seismic coda of the regional wave train to obtain magnitude estimates. This method worked well for estimating M_w for western U.S. events (Woods, 2002), and should perform similarly well for estimating m_{bLg} for earthquakes in the central and eastern U.S. Coda measurements have several advantages:

- 1) Coda amplitudes vary little with geologic structure and show little or no effect of azimuthal source radiation effects, thus allowing accurate single-station magnitude measurements;
- 2) Path-corrected coda amplitudes can be measured consistently over a large region, which makes comparison of source parameters for events throughout the U.S. possible, using a common methodology and station network;
- 3) Coda waves of large events can last for many minutes at local and regional distances, thus allowing the analysis of seismograms with clipped main arrivals.

A review of related coda-magnitude studies will be presented in the next section.

The third and last step, for events without available records to measure coda or other waveform information, is to develop revised inter-magnitude scaling relationship between m_{bLg} and M_w for ENA events, in order to provide a set of moment magnitudes for events in the region for use in ground-motion prediction and modeling studies, as M_w is preferable for such purposes. This same scaling relationship can then be applied to older, historical catalog events as well, in order to generate a M_w -based catalog.

In the following section the development of coda magnitude methods is reviewed, and the rationale for the method used in this study is given.

MEASURING CODA MAGNITUDES

Provided here is an overview of the development of coda-based magnitude scales, with particular attention paid to those on which the method in this study is premised.

which in turn was the basis for the coda magnitude used this study, the details of which are in the

Methodology section.

Coda magnitude measurements have a long history of use, and have been shown to give reliable, robust estimates of seismic source size. Herraiz and Espinosa (1987) give a general review of coda waves, and Herrmann (1975) also provides an overview of magnitude-measurement work in this area previous to his study -- the most contemporaneous one of these being Real and Teng's (1973) relation between M_L and short-period coda duration (time after P-wave first arrival) for southern California earthquakes, which they found to be:

$$M_L = C_0 + C_1 \cdot (\log \tau)^n + C_2 \cdot \Delta \quad (3)$$

with $n = 1$ for $M_\tau \leq 3.8$, and $n = 2$ for $M_\tau > 3.8$ events, where τ is the coda duration and Δ is epicentral distance. All references to log terms herein are with respect to log base ten. They noted that Lee *et al.* (1972), in a study of central Californian earthquakes, found a similar departure from a linear to a quadratic $\log(\tau)$ term in order to fit the duration data of larger magnitude events. Real and Teng speculated that this quadratic term for larger events is attributable to the fact that the M_L scale itself deviates non-linearly from either m_b or M_s for larger magnitude events.

Herrmann extended this application of coda duration measurement, by relating it directly to seismic moment, M_0 , using central and eastern U.S. events and short-period ($f = 1$ Hz) observations. He also found an upturn in the slope of the linear $\log M_0 - \log(\tau)$ relation at approximately $M_w = 3.8$ -- the same magnitude at which the empirical $M_L - \log(\tau)$ relationship, found by Real and Teng (1972), requires a quadratic term; in the case of regressing directly versus $\log(M_0)$, however, the exponent n in equation 3 was taken as unity by Herrmann. This change in the slope of the $M_w - M_C$ relationship was attributed to the convolved effect of source-spectrum corner frequency and instrument bandwidth -- that is, short-period measurements of coda underestimate the source spectrum of larger events with corner frequencies below the peak passband of the recording instrument. A number of other studies examining the relation between coda duration and seismic moment and local magnitude (Bakun and Lindh, 1977; Suteau and Whitcomb, 1979; Bakun, 1984a; and Bakun, 1984b) also found an empirical dependence of seismic moment on a quadratic $\log(\tau)$ term for events with $M > 4$.

The coda-duration magnitude relations described above are all empirically based, taking the general form of conventional magnitude equations, with the modification that a $\log(\tau)$ term replaces the usual \log amplitude ($\log(A)$) term. Duration in these studies has been defined as the time measured after a particular arrival (either P, S or Lg) at which the coda amplitude reduces to some minimal level, sometimes defined as the pre-transient signal-onset noise level, and sometimes defined as some slightly higher amplitude, usually the point at which the coda amplitude is some fraction of the peak S-wave amplitude, or at some multiple of the S-wave travel time, *e. g.* twice the S-wave travel time.

An alternative time measurement to use is lapse time (time measured origin time). Biswas and Aki (1984) use this measurement, in conjunction with coda amplitude, to determine seismic moment, for which their $\log(\tau)$ coefficient remains linear for all magnitude ranges. Lapse time was chosen because it is the appropriate time term for the coda scattering theory (see next paragraph for explanation) on which they base their magnitude measurement. As the approach applied in this study is a variation on this method, lapse time is the time measurement used.

Aside from the method of Biswas and Aki (1984), the other aforementioned studies included a distance term, although the distance dependence often was found to be weak. Aki and Chouet (1975) developed a description for coda waves in terms of scattering theory, based on the observations of Aki (1969) that local coda wave amplitude, in the 1-24 Hz passband, was primarily a function of coda lapse

time, and was found in these previous studies to be only weakly dependent on distance from the source. These coda waves are explained in terms of back-scattered waves -- primarily shear -- caused by heterogeneities distributed more or less uniformly in the crust. Rautian and Khalturin (1978) provided additional evidence supporting this interpretation of coda waves in an independent study. This theory implies that coda amplitude decay is a function of lapse time (time after origin) and that this curve is similarly shaped, *i. e.* parallel, for all events within a region, irrespective of the location of the source and the receiver; there is, however, a multiplicative offset factor related to the difference in source excitation and a receiver site correction. The validity of this characteristic of coda-wave amplitude decay has been demonstrated from observations from a variety of regions of the earth by the above authors.

There are certainly particular stations known to have anomalously long or ringing coda, caused by extreme receiver structure, *e. g.* thick sedimentary basins. Care must be taken when using such stations, and it would be better to forgo using such anomalous stations in general; however, most stations' receiver characteristics are suitable for application of this method.

Further, Aki (1980) showed that the attenuation (Q^{-1}) of S waves also has similar frequency dependence as that of coda waves; synthesizing these results Aki (1981) concluded that coda waves are S-to-S back-scattered waves. By this theory coda amplitude is represented by

$$A_c(\omega | \tau) = A_0 \tau^{-\gamma} e^{-\omega \tau 2Q} \quad (4)$$

in which A_0 is the source excitation, the $\tau^{-\gamma}$ term represents the effect of geometric spreading, and the second exponential term represents attenuation, which can be simplified with the substitution $b = \pi f / Q$. At lapse times sufficiently greater than the S arrival, and correcting for local geology site effects site effects, coda wave energy is observed to be homogeneously distributed in the crust (Aki, 1969; Aki and Chouet, 1975; and Mayeda *et al.*, 1992).

Mayeda (1993) applied this theory to NTS explosions recorded by the Lawrence Livermore National Laboratory Seismic Network, and established the following $m_b(Lg\ Coda)$ relationship to coda amplitude and lapse time:

$$m_b(Lg\ Coda) = \text{Log}_{10}[A_C(\tau)] + \gamma \cdot \log_{10}(\tau) + b \cdot \tau \cdot \log_{10}(e) + C \quad (5)$$

where the γ term represents geometric spreading, while b represents the anelastic attenuation term; $A_C(t)$ is the amplitude of the enveloped coda signal, and C is a constant. He found these magnitude estimates to be very robust and stable, yielding 75% to 80% variance reduction in single-station measurements over either $m_b(P_n)$ or m_{bLg} estimates. This formulation, used for this case in which source-receiver geometry did not deviate significantly between events recorded at any one station, worked well without incorporating a distance correction term, but the author acknowledged that for more general use distance needs to be accounted for as well, and that certain scattering models are capable of providing this.

Mayeda and Walter (1996), to this end, refined this method by measuring the coda envelope amplitude in different 20 consecutive bandwidths, between 0.05 and 10 Hz, and employing a 2-D scattering model (Shang and Gao, 1988) which determines the energy density $E(r,t)$, thus implicitly accounting for distance; in addition to which empirical Green's function corrections are made for each passband. This method proved very effective at estimating seismic moments; however, it requires digital data.

Given that the purpose of this study is to develop a magnitude measuring method applicable to older, analog data as well as to digital data, this latter method cannot be employed, as we desire one method to apply uniformly to digital and analog waveforms. Therefore we employ a hybrid of the Herrmann (1975) and Mayeda (1993) approaches of estimating magnitude (M_w) from time-domain seismogram measurements. To this end we employ the Mayeda formulation, but incorporate, as well, a distance-dependent term.

The epicentral distances involved in this study exceed the range to which the Aki-based coda scattering theory has been applied successfully in the past; further, the epicentral distances range widely, some as short as 100 km and others greater than 2000 km. Thus we are extending the application of coda magnitude measurements to far greater distances, which is necessary in regions with sparse station coverage; this is the case for the central and eastern U.S., given the available digital station coverage for the time window of events studied (see DATA section below).

DATA

Digital waveform data were collected for earthquakes from the USGS NEHRP CEUS catalog ($M \geq 3.5$) for the period 1988-1995; additionally, data were collected for later, larger ($M \geq 4.5$) events in order to provide more calibration events. Waveforms were obtained from IRIS DMS (see acknowledgements) and consist of broad-band, 20 samples/sec recordings. An effort was made to use as many stations as possible for each event, but we were limited by the number of available recording stations in the region. Figure 3 is a map of the central and eastern U.S., including the three seismic stations used (HRV, CCM, and SSPA) and the 110 events analyzed (this includes 9 earthquakes not in the CEUS catalog). For the time period examined the CEUS catalog contains 114 $m_{bLg} \geq 3.5$ events; however thirteen of these earthquakes had no available records from the network used. This is due partly to the geographic locations of the stations used and signal-to-noise-level considerations. Thus, 101 of the possible 114 CEUS events from this time period and magnitude range had their coda magnitudes calculated.

Stations used are ones currently recording digitally, but which were once analog-recording WWSN sites as well; hence the coda-magnitude calibration conducted here for digital data can directly be applied to analog data of the WWSN as well, thereby extending the time coverage from 1988 back to 1963. Calibration using the digital data, however, provides the most accurate measurements, which in turn will provide the best constrained coda-magnitude relationships for each station.

The seismograms were de-trended, had instrumental effects removed (deconvolved the instrument response) and were then convolved with a WWSP instrument. Their envelopes were then computed, smoothed over a 10-sec window and decimated to 1 sample/sec. This processing, using SAC (Seismic Analysis Code, Lawrence Livermore National Laboratory), produced in most cases smooth and well-defined coda curves, the exceptions being low signal-to-noise (SNR) records. The coda envelope curves were averaged over the three components (NS, EW and Vertical), when available. Coda amplitudes (nanometers or millimicrons) and their lapse times (sec) were picked by visual inspection. Measurement points were chosen from the envelope curves, which were past any large, distinct arrivals in the wavetrain, and where the slope of the coda curve (in log amplitude) was constant; this generally corresponded to the group velocity window of 0.75 to 3.0 km/s, with smaller group velocities associated with closer observations and *visa versa*.

Figure 4a provides an example waveform, its envelope, and the portion of the seismogram over which the coda amplitude is measured. For the purposes of directly applying this method to analog

WWSP data, Figure 4b compares the envelope to the absolute value of the time series (top and bottom panels, respectively); peak amplitude measurements of the time series are nearly equivalent to the envelope values, as is expected. Thus for the purposes here, these two types of measurements -- either digital smoothed envelopes or direct time-domain amplitude measurements -- can be used interchangeably, since the difference between them is negligible. These coda measurements were then used to estimate seismic moment as described in the following section.

METHODOLOGY and RESULTS

As mentioned previously, we are applying a variation of the Mayeda (1993) method to determine coda magnitude by also incorporating a distance factor into the relationship between the coda amplitude and the source factor; for this a distance dependence inversely proportional to some power of Δ , the epicentral distance, is assumed; thus equation 4 is modified to become:

$$A_c(\omega | \tau) = A_0 \cdot \tau^{-\gamma} \cdot \Delta^{-n} \cdot e^{-\omega\tau 2Q}, \quad (6)$$

where, again, $2\omega Q$ can be replaced by the term b . Taking the logarithm of equation 5, rearranging terms, and taking $\log(A_0)$, the log of the source factor, to be equivalent to M_C , yields the following expression for coda magnitude:

$$M_C = \log(A_c) + \gamma \log(\tau) + b \cdot \tau + n \cdot \log(\Delta). \quad (7)$$

Here a further constant, a_0 , can be included as a station correction term. Since the coda magnitudes are calibrated with respect to m_{bLg} , and hence tied to it, the coda magnitudes obtained in this study will be referred to hereafter as m_{bLg} (coda) or coda m_{bLg} .

To calibrate coda m_{bLg} (equation 7), direct m_{bLg} values were compiled for digitally-recorded events from the CEUS catalog, *i. e.* those occurring between 1988 and 1995, as well as more recent ones (1995+), resulting in 112 potential "master events"; the number available for any single station varied, depending on the station's recording history and the signal-to-noise level of observations for the various events, the latter feature also being a function of magnitude and epicentral distance. In the initial effort to also calibrate coda magnitude to M_w , seismic moments were also collected; however the available number of them was small, making it infeasible to do so; none the less these M_w 's were compiled, and make up the 1988+ portion of the events in Table 3, which also cites the reference source.

We investigated the behavior of coda lapse time and amplitude with respect to this equation for the available broadband digital IRIS-station records from HRV, CCM and SSPA. As this expression has transcendental terms, it cannot be linearized for solving. Consequently, we used a simple grid-search error minimization approach to obtain the best-fitting parameters; first the general range of values, between stations, for each parameter was found; then the best fitting parameters for the three stations were determined within these ranges. For these purposes additional events, not in the CEUS catalog, were included in order to increase the size of the data sets used for determining these parameters; these events are also included in the inter-station comparisons of coda-based $m_b LG$ values to be discussed below.

Gamma (γ), the log lapse-time coefficient, was first determined to range between 0.4 and 0.8 for all three stations; consequently, we chose to take a weighted average of 0.65 for each station. With this parameter established, consistent, stable values were found for the other terms as well; n , the log-distance coefficient was found to be 0.25 for each station; a_0 , the constant term, was 7.3, 7.4, and 7.5

for CCM, SSPA and HRV respectively, suggesting relatively small inter-station offsets; while b , the linear lapse-time coefficient, varied the most, ranging between $5.7e-4$, $8.5e-4$ and $9.6e-4$ for HRV, SSPA and CCM respectively. These are the final parameter values used to obtain coda-magnitude m_{bLg} for the earthquakes analyzed.

The final coda m_{bLg} 's are provided in Table 2; when more than one station recording was available for an event, a network average was determined for it. This set of events includes non-CEUS catalog earthquakes used to fill out the data set for statistical robustness. Forty-five events had magnitude measurements from more than one station, yielding an average inter-station magnitude standard deviation of 0.085. Inter-station regressions also were performed.

Figure 5 compares CCM to HRV; the top (a) is for an unconstrained regression, the bottom (b) is for a fixed slope of unity. The expected slope of unity falls within 2σ of the best-fitting free slope; for this case, the offset, 0.011, is statistically insignificant, suggesting a one-to-one scaling relationship between the two stations' magnitude estimates. In this case there are 40 data. The standard error of estimate is 0.16. This number is fairly high in comparison to the inter-station error found by Mayeda (1993); however, it must be kept in mind that his study used events from one site, thus removing any appreciable distance effect, and the stations used were relatively close together (within 600-800 km of each other), whereas HRV and CCM, for example, are 1737 km apart. It is not surprising then, that the inter-station magnitude correlation for this is somewhat degraded; still such relatively small differences between single-station magnitude estimates made at such distances -- and for events throughout a wide geographic region -- is still impressive and suggests that this is a stable method to determine regional magnitude for sparse seismic networks.

The station SSPA only began running in December, 1994, and consequently only recorded a few CEUS-catalog earthquakes; therefore most of the events used for this station were post 1995, i.e. past the CEUS catalog time window, and so make up the majority of the events used in inter-station magnitude comparisons. Figure 6 compares HRV and SSPA m_{bLg} 's for the nine earthquakes recorded by both stations; the top panel is for the unconstrained regression, the lower is for a fixed slope of unity. In this case the unconstrained regression, with a slope of 1.02, yields a significantly smaller standard error of estimate (0.10 vs. the fixed-slope resulting error of 0.13); however, a slope of unity still falls nearly within the $2-\sigma$ range of the unconstrained result, being outside the error range of the free-slope result by less than 0.006. That so few data are available skews the statistics; hence the significantly larger standard error of estimate for the fixed slope of unity case. It is expected that a larger data set would confirm that a scaling relationship between the two stations' magnitudes is close to one-to-one, i.e. a slope of unity. As it stands, the offset between HRV and SSPA m_{bLg} 's is 0.033, which is smaller than its associated estimated error (0.083).

Figure 7 provides the analogous regression comparison between CCM and SSPA m_{bLg} 's. In this case the fixed slope of unity regression (lower panel) falls within the $2-\sigma$ range of the unconstrained result, and for this the standard estimate of error is slightly less; again the offset in the two stations' m_{bLg} 's is statistically insignificant for the fixed-slope relationship. Once again the number of mutual m_{bLg} 's for the two stations is small; a larger number would be desired for a more statistically robust result. None the less, the three sets of inter-station regression comparisons suggest that the m_{bLg} estimates are consistent between the stations and that all follow one-to-one scaling relationships.

The network-averaged (for cases with more than one recording station) coda m_{bLg} 's are regressed with respect to their CEUS m_{bLg} counterparts in Figure 8. The fixed-slope ($m = 1$) result (b) falls within the error bounds of the unconstrained (a) result, although the standard estimate of error is slightly larger in the former case. The most conspicuous outlying datum point is of the Saguenay

earthquake (11/25/88); its CEUS m_{bLg} is 5.80, whereas its coda-based m_{bLg} is 6.18 (see table 2). This is not a completely surprising result, however, as the actual (direct) m_{bLg} estimate for this event is 6.54, whereas teleseismic m_b 's for the event are in the range 5.8-5.9 -- as is its M_w ; hence the CEUS m_{bLg} value is based on these converted, lower magnitude values, whereas the coda m_{bLg} value would tend to be closer to the actual m_{bLg} value as it is also determined from regional short-period data.

Thus, as the coda-based m_{bLg} measurements appear to be self-consistent, with even single-station magnitude estimates being robust and accurate, we infer that those for the 102 CEUS earthquakes (and nine additional events) in Table 2 are consistent and accurate.

Unfortunately this is still a small portion of the CEUS events in the instrumented time range (1963+); hence other methods to revise the m_{bLg} estimates in this catalog are still of considerable interest. Further, as discussed already, M_w provides a better measure of the long-period (LP) source spectrum than m_{bLg} , and so is more useful for quantifying seismic sources in ground motion studies. Therefore, a better direct relationship between M_w and m_{bLg} for central and eastern North American earthquakes is of great importance. To this end, we compiled direct m_{bLg} and M_w estimates for eastern North America (ENA), in order to derive more robust and comprehensive scaling relationships between these two magnitude systems

The m_{bLg} 's and M_w 's come from a number of published studies; all m_{bLg} values were directly obtained, *i.e.* not converted, or inferred from teleseismic m_b values or any other magnitude scales. The events used include those in the CEUS catalog, but are not limited to them, in order to create as large and comprehensive a M_w - m_{bLg} pair data set as possible. The M_w values fall into two general categories: direct long-period (LP) measurements involving inversion of regional surface-wave and/or body-wave waveforms (Herrmann, 1979; Nuttli, 1983, Somerville *et al.*, 1987, Zhao and Helmberger, 1989; and Saikia *et al.*, 1998) and Lg -spectra moments, which are short period (SP) in nature (Street *et al.*, 1975; Street and Turcotte, 1977; and Street, 1984); the latter moments or M_w 's may be biased at larger magnitudes due to the frequency range of the Lg measurements made and the corner frequency of larger magnitude events; therefore some care must be taken when analyzing the larger Lg -based M_w estimates.

Figure 9 shows the regression results for M_w (LP) vs. m_{bLg} : the top panel being the unconstrained regression and the lower panel being the fixed-slope ($m = 1$) result. A slope of unity is within the error bounds of the unconstrained case; however, in this case there is a statistically significant offset of 0.163 in the scaling relationship; still M_w and m_{bLg} seem to scale at the same rate. There appears to be no saturation of the m_{bLg} values relative to M_w ; if anything, the opposite may be the case, with M_w being larger than m_{bLg} for all the larger ($m_{bLg} > 6$) events, although this effect is small.

Figure 10 shows analogous regression results for M_w (SP) vs. m_{bLg} ; here the data set is nearly four times larger than for the LP M_w case (201 events compared to 51), and the magnitude range is wider (compare the axes ranges of Figure 9 and 10). The free-slope regression yields a well-constrained slope of 0.906; however, the data set is skewed towards the magnitude range of 3 to 5, and so the scaling-relationship slope at larger magnitudes is not so well established. Fixing the scaling slope at unity results in a 0.413 magnitude offset between M_w and m_{bLg} ; this relationship holds well for $m_{bLg} > 3$ events.

Next we combined the two types of M_w data, *i.e.* LP and Lg -based; the regression results for this combined population are provided in Figure 11, again the top panel is the unconstrained result, and the bottom panel is the fixed-slope ($m = 1$) result. The constrained slope results falls within the error

bounds of the unconstrained regression result; thus a self-similar scaling relationship is obtained. In both cases this yields an offset of between 0.36 and 0.40 magnitude units. This result is interesting because it suggests that M_w is, indeed, directly transportable between the western and the central and eastern United States, the details of which are provided in the Discussion section.

Finally, we examined the possibility of a non-constant scaling relationship, *i.e.* one for which the slope changes at some point in the magnitude range. Figure 12 shows the results; the top panel is for $m_{bLg} \leq 5$ events, and the bottom panel is for $m_{bLg} \geq 4.75$ ones; note the difference in scale range between the two plots (the top one, for larger, events being between magnitude 2 and 6, while the lower one, for smaller events being between magnitude 3 and 7. For the case of the smaller events the slope of the 2- σ confidence line is 0.928 ± 0.049 , thus less than unity in any case; whereas for the larger events a more poorly constrained slope of 1.165 ± 0.175 is obtained, for which a slope of unity falls within these error bounds.

The relatively small standard error of estimate for the smaller events, 0.22 magnitude units, slightly smaller than the 0.23 for the entire data set, suggests that the M_w - m_{bLg} scaling relationship, indeed, may have a slope slightly less than unity for $m_{bLg} \leq 5$ events; however the relatively large value standard error of estimate for the $m_{bLg} \geq 4.75$ events suggests that this latter result is poorly constrained. Hence we assume that the fixed-slope ($m = 1$) result for the combined data set (Figure 11) provides the best general scaling relationship between M_w and m_{bLg} , *i.e.* $M_w = m_{bLg} - 0.36 \pm 0.03$.

DISCUSSION

The coda m_{bLg} method applied here to central and eastern North American earthquakes is a variation of the one developed by Woods (2002) using western U.S. earthquakes, the difference being that what was a linear distance term in the previous study's coda magnitude relationship is a log-distance term in the present one. In early trials using the new formulation, the log-distance term was found to provide more stable and consistent solutions to the coefficients of the coda magnitude (equation 7) than the linear distance term in the analogous equation (Δ instead of $\log(\Delta)$); not only did this stability and consistency in the coefficients hold between stations, but the log-distance coefficient was always positive, whereas the linear distance coefficient in the older version was for most stations negative, implying increasing coda with distance -- an unrealistic phenomenon; hence, the log-distance formulation provides a physically more reasonable model for the dispersion of coda energy.

Also physically more reasonable is the result found here that the factor γ was determined to be 0.65 for all three stations, for in the relationship between coda amplitude to the source factor (eq. 3), Mayeda has remarked that the form of the $\tau^{-\gamma}$ term corresponds to geometric spreading and that of $e^{-\omega\tau 2Q}$ to anelastic attenuation. Mayeda found a γ of 2.5 to fit his data; however a more appropriate exponent for geometric spreading would be between 0.5 for surface waves and 1.0 for body waves. This study's result of 0.65 for all stations is intermediate between these two physical bounds, and is closer to that of surface waves; which is expected since scattered energy within the crust should behave more as multiply-scattered surface waves than as body waves, which would tend to leak out of the crustal waveguide with greater propagation distance, thus becoming but a small component of coda energy.

The standard estimates of error for the inter-station coda m_{bLg} regressions range between 0.13 and 0.16, which are larger than those obtained by Mayeda using a similar coda magnitude measuring method. However, his study, using NTS explosions, relied on distance-invariant -- or nearly so -- observations, thereby avoiding any distance correction. Further, the sources used -- explosions --

generally generate relatively spherically symmetric wavefields, whereas earthquakes, with double-couple style mechanisms, have azimuthally dependent radiation patterns that can appreciably effect coda amplitude and lapse-time measurements; only the larger explosions with large tectonic release, *i.e.* a high f factor (the ratio of explosion to double-couple, *i.e.* earthquake, long-period source spectrum) would give rise to similar such azimuthal radiation patterns in generating coda. Therefore it is not surprising that the spatially-varied earthquake data set, even with distance corrections incorporated, yields larger standard error estimates for this case, approximately twice as large as for the constant-distance case of Mayeda (1993).

Also, this study makes use of more ($R > 600$ km) regional seismograms than have past coda-magnitude studies, including that of Mayeda (1993); this entailed extending lapse-time measurements, as well, to times as great as 600 to 900 sec. The window chosen, as late in the coda as possible given noise-level considerations, corresponds to group velocities that, on average, grow with epicentral distance. For distances less than 300 km, the range was approximately between 0.75 and 1.3 km/s. Lapse-time measurements of less than 100 sec. underestimated the magnitude; consequently none were not used, but rather measurements were made in the later coda. Group velocities for the coda in the intermediate distance range ($300 \text{ km} < R < 600 \text{ km}$) vary between 1.3 and 2.0 km/s. These two types of observations are in agreement with those of Mayeda (1993). Additionally, coda wave-train group velocities for the more distant ($R > 600 \text{ km}$) events range between 2.0 and 3.0 km/s. Magnitude estimates made from these more distant observations are consistent with nearer ones from other stations. Thus the coda magnitude measurement method has been extended to significantly more distant observations, which require accurate distance corrections; that the variance in the inter-station comparisons is larger than for a more constricted (distance-wise) data set, is not surprising.

We attribute this increase in coda-wave group velocity with distance to two factors: the first is the deeper sampling of the crust by scattered waves at greater distances, the second is near-receiver scatter from deeper-sampling direct phases and wavetrains for longer propagation paths. We favor the second mechanism as the primary effect, but have no direct evidence to support this, but rather it is based upon the author's experience in modeling regional wavetrains, wherein significant secondary arrivals are generated near a receiver, particularly one with a low-velocity layer beneath it.

The slope of the scaling relationship in each of the three inter-station unconstrained regressions lie about unity, with fixed-slope ($m = 1$) results falling within the $2\text{-}\sigma$ error bars of the unconstrained slopes. The events available to analyze are skewed in number towards smaller ($m_{bLg} < 4.5$) earthquakes, so that the free-slope regression scaling equations are biased towards the distribution of smaller events in particular. We attribute the deviation from unity in the slope of these inter-station scaling relations to these biases, and because the fixed-slope results fall within the $2\text{-}\sigma$ unconstrained estimates, with standard errors of estimated being nearly equivalent, we take the m_{bLg} relationships to be one to one (*i.e.* with slope = 1) in all cases.

The data set, consisting of records from only three stations, some of which only came online after the beginning of the time window of events examined (CCM: 1989 onwards, SSPA: 1994 onwards), provides multiple Lg coda observations for only more recent events, and even then only when two or more stations had available good signal-to-noise-ratio (SNR) observations for an event; consequently many of the network-averaged m_{bLg} are often single-station estimates. None the less the coda m_{bLg} vs. CEUS m_{bLg} regression result has a standard error of estimate of 0.20 -- slightly larger than those for the inter-station m_{bLg} regression. Given the consistently smaller errors for the inter-station comparisons, we infer that this slightly larger error is due to inaccuracies in CEUS magnitude values. These inaccuracies are likely due to converted m_{bLg} values used to generate the CEUS catalog, *i.e.* converted from other magnitude types using inappropriate conversion relationships.

To better determine the inter-magnitude scaling relationships between m_{bLg} and other magnitude scales, empirical regressions, using the CEUS m_{bLg} magnitudes in conjunction with those of another particular magnitude scale, were performed. This resulted in inter-magnitude scaling relationships, or magnitude conversion equations, different from those used by Mueller *et al.* (1997). For instance, in regressing M_w vs. m_{bLg} (CEUS), for all available such historical events (Figure 1) -- that is, including those for older, analog-recorded events -- yielded the result: $M_w = m_{bLg}$ (CEUS) - 0.202, which differs from the relation $M_w = m_{bLg}$ (CEUS) used by Mueller *et al.* (1997).

To better understand which, if either, relationship is correct, we first look at pertinent inter-magnitude relationships found in other studies, in particular those between M_w , m_{bLg} , m_b (tel) and M_L , and how these magnitude relations compare between the western U.S. and central and eastern North America. First of all, it should be remembered that m_{bLg} was devised and developed to link a regional magnitude scale directly to teleseismic m_b ; in particular, this was done for the central U.S. (Nuttli, 1973). Chung and Bernreuter (1981) illustrate, however, that teleseismic m_b can itself have regional biases, due to differences in mantle attenuation beneath the source and/or the receiver region, and that, in particular, there appears to be a bias in m_b between the eastern and western U.S., whereby:

$$m_b(\text{west}) = m_b(\text{east}) - 0.33 \quad (8)$$

where the offset, -0.33, is an approximate Δm_b inferred by their modeling of upper-mantle attenuation differences, which is in line with other studies' observations.

Previously, in a study of the western U.S., Woods (2002) found, regressing surface-wave determined M_w 's (Thio and Kanamori, 1995) and Southern California Network M_L 's for 262 southern California earthquakes that $M_w = M_L$ in the range: $3 < M < 6.8$. Ebel (1982) determined M_L 's for northeastern U.S. events, using an attenuation term appropriate to the region. We regressed these M_L with m_{bLg} for these events; the results are shown in Figure 13. Although the unconstrained scaling relationship slope is less than unity -- 0.794 ± 0.153 -- the error is fairly large and the fixed-slope ($m = 1$) result's error is not appreciably larger; further, the scattered outlying data about $m_{bLg} = 3.0$, which skew the regression result, warrant a fixing of the slope for the most appropriate scaling relationship; hence, for the purposes here we approximate the M_L - m_{bLg} relationship for ENA as:

$$M_L = m_{bLg} - 0.423. \quad (9)$$

This result is in contrast to that inferred by Herrmann and Nuttli (1982) that $M_L = m_{bLg}$ for earthquakes in any one region; the latter study inferred this result only for western U.S. earthquakes and stations, whereas the former was obtained directly from ENA events.

As Ebel (1982) formulated M_L , in his study of northeastern North American earthquakes, using the same definition as has been historically used for western U.S. earthquakes -- the only difference being the appropriate change in the attenuation coefficient for the distance correction -- M_L should also scale equivalently to M_w , as was shown it does for the western U.S. (Woods, 2002), hence:

$$M_w \approx m_{bLg} - 0.423 \quad (10)$$

for ENA as well. This is close to the direct relation obtained in this study for M_w and m_{bLg} (Figure 11) for a compilation of ENA earthquakes:

$$M_w = m_{bLg} - 0.363. \quad (11)$$

Given the approximations made by assuming unit-slope scaling relationships between magnitude types, the constant, or offset, term in equations 10 and 11 is in relatively close agreement; this offset is also quite similar in value to that found between m_b (west) and m_b (east) (equation 8). Thus there seems to be a consistency in offset of empirical magnitude scales between the eastern and western U.S.

We infer then that equation 11 is the appropriate M_w - m_{bLg} relationship for ENA, and should be used for converting between the two magnitude scales in compiling any comprehensive magnitude catalog for the eastern United States. Similarly, equation 9 should be used for conversions between M_L and m_{bLg} for the region.

That the $M_w - m_{bLg}$ difference is significantly off from that found directly regressing M_w with m_{bLg} for master events, *i.e.* ones with direct M_w estimates, in the CEUS catalog (Figure 1), suggests systematic differences in the weighted, converted m_{bLg} values in the CEUS catalog, which are most likely due to the magnitude conversions, or scaling relations, used to generate the catalog.

CONCLUSIONS

We have developed a method for estimating m_{bLg} from near- and far-regional coda amplitudes and lapse-times, and applied it to $m_{bLg} \geq 3.5$ earthquakes in ENA, thereby lowering the magnitude threshold of the method in comparison to a related study of western U.S. earthquakes (Woods, 2002). Reducing the magnitude threshold was necessary because of the relatively sparse seismicity for ENA relative to that of the western U.S., and was possible because of the lower seismic attenuation of the ENA, which yields improved SNR observations for smaller events. Inter-station comparisons of these coda m_{bLg} 's yield relatively low standard error of estimates, suggesting that the method gives consistent and robust single-station estimates of m_{bLg} .

Although these coda m_{bLg} measurements were only made on digital seismograms for 1988+ earthquakes, the simple time domain measurement used can be applied to analog records for older recorded earthquakes as well, in particular for short-period WWSN seismograms of 1963+ events. These coda-based m_{bLg} 's have been compiled (see Table 2) for updating the CEUS seismic hazard catalog. They are available electronically, for interested parties to update the NEHRP CEUS catalog, as well as for general use of the seismological community.

Ideally M_w would be a better means to quantify the long-period source spectrum of earthquakes, for predicting ground motions; however, there were not enough events in the NEHRP CEUS catalog for which independent M_w 's were available to perform this calibration. Instead we compiled M_w 's and m_{bLg} 's for central and eastern U.S. earthquakes in order to determine a comprehensive scaling relationship between the two magnitudes, which can be used to convert raw magnitudes to one universal type for any future revised NEHRP CEUS catalog (equation 11). This result can be used to convert the CEUS catalog m_{bLg} magnitudes to M_w , a more useful quantity for predicting and modeling strong ground motions, and appears to be appropriate throughout the magnitude range $2 < m_{bLg} < 6.5$.

Similarly, a new M_L - m_{bLg} relationship (equation 9) was empirically determined for eastern North American earthquakes, which is more appropriate for converting between the two magnitude scales, in particular for revising the CEUS catalog. This result also suggests that for ENA the M_L and M_w scaling relationship is one to one, *i. e.* $M_L \approx M_w$; this is the same relation which holds for western U.S. earthquakes.

REFERENCES

- Aki, K., 1969. Analysis of the seismic coda of local earthquakes as scattered waves, *J. Geophys. Res.* **74**, 615-631, 1969.
- Aki, K. and B. Chouet, 1975. Origin of coda waves: source, attenuation, and scattering effects, *J. Geophys. Res.* **80**, 3322-3342.
- Aki, K., 1980. Attenuation of shear waves in the lithosphere for frequencies from 0.05 to 25 Hz, *Phys. Earth Planet. Int.* **21**, 50-60.
- Aki, K., 1981. Attenuation and scattering of short-period seismic waves in the lithosphere, in *Identification of Seismic Sources -- Earthquakes or Underground Explosion*, E. S. Husebye and S. Mykkeltveit, Editors, D. Reidel Publishing Co., Dordrecht, The Netherlands.
- Atkinson, G. M., 1993. Earthquake Spectra in eastern North America, *Bull. Seism. Soc. Am.* **83**, 1778-1798.
- Bakun, W. H. and A. G. Lindh, 1977. Local magnitudes, seismic moments, and coda durations for earthquakes near Oroville, California, *Bull. Seism. Soc. Am.* **67**, 615-629.
- Bakun, William H., 1984a. Seismic moments, local magnitude and coda-duration magnitudes for earthquakes in central California, *Bull. Seism. Soc. Am.* **74**, 439-458.
- Bakun, William H., 1984b. Magnitudes and moments of duration, *Bull. Seism. Soc. Am.* **74**, 2335-2356.
- Biswas, N. N. and K. Aki, 1984. Characteristics of coda waves: central and south-central Alaska, *Bull. Seism. Soc. Am.* **74**, 493-507.
- Boatwright, John, 1994. Regional propagation characteristics and source parameters of earthquakes in northeastern North America, *Bull. Seism. Soc. Am.* **84**, 1-15.
- Chung, D. H. and D. L. Bernreuter, 1981. Regional relationships among earthquake magnitude scales, *Rev. Geophys. and Space Phys.* **19**, 649-663.
- Ebel, John E., 1982. M_L Measurements for northeastern United States earthquakes, *Bull. Seism. Soc. Am.* **72**, 1367-1378.
- Electric Power Research Institute (EPRI), 1986. "The Earthquakes of stable regions" Volume 1: Assessment of large earthquake potential, *Prepared by: U. Memphis Center for Earthquake Research and Information, Memphis, TN.; Geomatrix Consultants, San Francisco, CA; CAC, Portola Valley, CA.* page: 3-25.
- Frankel, A., 1995. Mapping seismic hazard in central and eastern United States, *Seism. Res. Letts.* **66**, 8-21.
- Frankel, A., C. Mueller, T. Barnhard, D. Perkins, E. V. Leyendecker, N. Dickman, S. Hanson, and M. Hopper, 1996. Interim National Seismic Hazard Maps: Documentation, U.S. Geological Survey, Open-File Report 96-S32 (<http://gldage.cr.usgs.gov/eq/hazmapsdoc/>), 100p.

- Herraiz, M. and A. F. Espinosa, 1987. Coda waves: a review, *Pure and Applied Geophys.* **125**, 499-577.
- Herrmann, R. B. 1975. The Use of duration as a measure of seismic moment and magnitude, *Bull. Seism. Soc. Am.* **65**, 899-913.
- Herrmann, R. B., 1979. Surface wave focal mechanisms for eastern North American earthquakes with tectonic implications, *J. Geophys. Res.* **84**, 3543-3552.
- Herrmann, Robert B., and Otto W. Nuttli, 1982. Magnitude: The Relation of M_L to m_{bLg} , *Bull. Seism. Soc. Am.* **72**, 389-397.
- International Seismological Center (ISC), 2001. *On-line Bulletin*, <http://www.isc.ac.uk/Bul>, Internatl. Seis. Cent., Thatcham, UK.
- Kanamori, H., 1977. The energy release in great earthquakes, *J. Geophys. Res.* **82**, 2981-2987.
- Mayeda, K., S. Koyanagi, Hoshiya, K. Aki and Y. Zeng, 1992. A comparative study of scattering, intrinsic, and coda Q^{-1} for Hawaii, Long Valley and central California between 1.5 and 15.0 Hz, *J. Geophys. Res.* **97**, 6643-6659.
- Mayeda, K., 1993. $m_b(LgCoda)$; A stable single station estimator of magnitude, *Bull. Seism. Soc. Am.* **83**, 851-861.
- Mayeda, K. and W. Walter, 1996. Moment, energy, stress drop, and source spectra of western United States earthquakes from regional coda envelopes, *J. Geophys. Res.* **101**, 11,195-11,208.
- Mueller, C., H. Hopper and A. Frankel, 1997. Preparation of earthquake catalogs for the National Seismic Hazard Maps: Contiguous 48 States. U.S. Geological Survey Open-File Report 97-464 (<http://geohazards.cr.usgs.gov/eq/of97-464>).
- Nuttli, O. W., 1973. Seismic wave attenuation and magnitude relations for eastern North America, *J. Geophys. Res.* **78**, 876-885.
- Nuttli, O. W., 1983. Average seismic source-parameter relations for mid-plate earthquakes, *Bull. Seism. Soc. Am.* **73**, 519-535.
- Rautian, T. G. and V. I. Khalturin, 1978. The use of the coda for determination of the earthquake source spectrum, *Bull. Seism. Soc. Am.* **68**, 923-948.
- Saikia, C. K., P. G. Somerville, H. K. Thio, N. F. Smith, A. Pitarka, and B. B. Woods, 1998. Crustal structure and ground motion models in the eastern and central United States from National Seismic Network data, *U.S. Nuclear Regulatory Commission Report, NUREG/CR-6593*, Woodward-Clyde Federal Services, Pasadena, CA.
- Shang, T. and L. S. Gao, 1988. Transportation theory of multiple scattering and its application to seismic coda waves, *Sci. Sinica (Series B)*, **31**, 1503-1514, 1988.

- Somerville, P. G., J. P. McLaren, L. V. LeFevre, R. W. Burger, and D. V. Helmberger, 1987. Comparison of source scaling relations of eastern and western North American earthquakes, *Bull. Seism. Soc. Am.* **77**, 322-346.
- Street, R. L., R. B. Herrmann and O. W. Nuttli, 1975. Spectral characteristics of the *Lg* wave generated by central United States earthquakes, *Geophys. J. R. astr. Soc.* **41**, 51-63.
- Street, R. L., F. T. Turcotte, 1977. A Study of northeastern North American spectral moments, magnitudes and intensities, *Bull. Seism. Soc. Am.* **67**, 599-614.
- Street, R. L., 1984. Some recent *Lg* phase displacement spectral densities and their implications with respect to the prediction of ground motions in eastern North America, *Bull. Seism. Soc. Am.* **74**, 757-762.
- Suteau, A. M. and J. H. Whitcomb, 1979. A local earthquake coda magnitude and its relation to duration, moment M_0 and local Richter magnitude M_L , *Bull. Seism. Soc. Am.* **69**, 353-368.
- Thio, H. K. and H. Kanamori, 1995. Moment-tensor inversions for local earthquakes using surface waves recorded at TERRASCOPE, *Bull. Seism. Soc. Am.* **85**, 1021-1038.
- Woods, B. B., 2002. Revising moment-magnitude earthquake catalogs for use in generating the national seismic hazard maps, *USGS Annual Technical Report*, URS Group, Inc., Pasadena, CA.
- Zhao, L. S. and D. V. Helmberger, 1991. Broadband modeling of the 25 November 1988 Saguenay earthquake at regional distances, *Geophys. J. Int.* **105**, 301-312

ACKNOWLEDGEMENTS:

This research supported by the U.S. Geological Survey (USGS), Department of the Interior, under USGS award number 01-HQ-GR-0158. The views and conclusions contained in this document are those of the authors and should not be interpreted as necessarily representing the official policies, either expressed or implied, of the U.S. Government. The facilities of the IRIS Data Management System, and specifically the IRIS Data Management Center, were used to access waveform data and metadata required in this study. The IRIS DMS is funded through the National Science Foundation and specifically the GEO Directorate through the Instrumentation and Facilities Program of the National Science Foundation under Cooperative Agreement EAR-0004370.

BIBLIOGRAPHY OF PROJECT-RELATED PUBLICATIONS AND PRESENTATIONS:

Woods, B. B., 2001. Coda-based m_{bLG} magnitudes for eastern North American earthquakes, *EOS. Trans. AGU*, **82** (48), Fall Meeting Suppl., Abstract S61A-25.

Woods, B. B., 2003. Determining coda m_{bLg} magnitudes for central and eastern North American earthquakes, and a new m_{bLg} - M_w scaling relationship for the region, submitted to: *Bull. Seism. Soc. Am.* (A redacted version of this report).

Table 1: CEUS Catalog Earthquakes with Moment (M_W) estimates						
Date	Hr:Min	Latitude	Longitude	M_W	m_{bLg}	Reference
1962/2/2	6:43	36.370	-89.510	4.21	4.30	Herrmann, 1979
1963/3/3	17:30	36.640	-90.050	4.64	4.80	Herrmann, 1979
1965/8/14	13:13	37.230	-89.310	3.58	3.80	Herrmann, 1979
1965/10/21	2:04	37.480	-90.940	4.58	4.90	Herrmann, 1979
1966/1/1	13:23	42.840	-78.250	4.25	3.90	Herrmann, 1979
1967/6/4	16:14	33.550	-90.840	4.27	4.30	Herrmann, 1979
1967/6/13	19:08	42.840	-78.230	4.06	3.90	Herrmann, 1979
1967/7/21	9:14	37.440	-90.440	4.02	4.60	Herrmann, 1979
1968/11/9	17:01	37.910	-88.370	5.31	5.50	Herrmann, 1979
1969/1/1	23:35	34.990	-92.690	4.31	4.40	Herrmann, 1979
1969/11/20	1:00	37.450	-80.930	4.52	4.60	Herrmann, 1979
1970/11/17	2:13	35.860	-89.950	4.08	4.40	Herrmann, 1979
1972/9/15	5:22	41.640	-89.370	4.10	4.40	Herrmann, 1979
1973/6/15	1:09	45.310	-71.120	4.47	4.80	Herrmann, 1979
1973/11/30	7:48	35.890	-83.990	4.06	4.60	Herrmann, 1979
1974/2/15	13:33	36.400	-100.690	4.34	4.50	Herrmann, 1979
1974/4/3	23:05	38.550	-88.070	4.32	4.70	Herrmann, 1979
1975/6/13	22:40	36.540	-89.680	3.72	3.90	Herrmann, 1979
1975/7/9	14:54	45.500	-96.100	4.27	4.60	Herrmann, 1979
1976/3/25	0:41	35.580	-90.480	4.60	4.90	Herrmann, 1979
1979/8/19	22:49	47.670	-69.900	4.73	4.60	Somerville et al., 1979
1980/7/27	18:52	38.190	-83.890	5.03	5.20	H, U, Somerville et al., 1979
1982/1/9	12:53	47.000	-66.600	5.41	5.70	H, U, Somerville et al., 1979
1983/10/7	10:18	44.030	-74.310	4.90	5.20	H, U, Somerville et al., 1979
1984/9/8	0:59	44.138	-106.110	4.91	5.03	HVD, USGS
1984/10/18	15:30	42.317	-105.735	5.30	5.44	HVD, USGS
1988/11/25	23:46	48.117	-71.183	5.79	5.80	H, Zhou & Helmberger, 1993
1989/11/16	9:24	46.570	-76.590	3.54	4.00	Boatwright, 1994
1990/10/7	8:47	46.320	-75.190	3.56	3.90	Boatwright, 1994
1990/10/19	7:01	46.437	-75.576	4.49	4.93	Boatwright, 1994
1994/1/16	1:49	40.330	-76.037	4.57	4.60	Saikia et al., 1998

Table 1. CEUS catalog earthquakes with independent moment estimates (H/HVD = Harvard CMT catalog, U/USGS = USGS moment tensor solution (NEIC catalog)). m_{bLg} 's are CEUS catalog values.

Table 2: Network-averaged coda m_{bLg}						
Date	Hr:Min	Longitude	Latitude	m_{bLg}	σ	n
88/01/14	17:23	-89.621	46.5590	4.20	-	1
88/03/10	14:42	-75.716	46.3410	3.55	-	1
88/04/14	23:37	-81.987	37.2380	3.82	-	1
88/08/09	13:57	-74.955	44.9950	3.21	-	1
88/09/07	02:28	-83.878	38.1430	4.54	-	1
88/10/20	13:09	-71.158	44.5390	3.92	-	1
88/11/14	06:15	-70.386	44.4240	3.81	-	1
88/11/23	09:11	-71.3217	48.1274	4.52	-	1
88/11/25	23:46	-71.183	48.1170	6.18	-	1
88/11/26	03:38	-71.4785	48.2624	3.88	-	1
88/12/28	06:28	-69.342	44.5140	3.74	-	1
89/01/01	17:55	-67.357	49.2640	3.92	-	1
89/03/11	08:31	-69.900	47.7000	4.07	-	1
89/04/06	02:35	-71.144	44.5110	3.34	-	1
89/04/10	18:12	-82.068	37.1360	4.06	-	1
89/04/27	16:47	-89.768	36.0060	4.38	0.11	2
89/05/14	00:16	-89.710	36.7400	3.97	-	1
89/06/08	18:18	-99.477	39.1650	4.13	-	1
89/08/10	21:17	-65.820	46.6500	3.53	-	1
89/08/20	00:03	-87.645	34.7360	3.85	-	1
89/09/14	17:31	-89.620	36.5450	3.31	-	1
89/11/16	09:24	-76.590	46.5700	3.79	0.10	2
90/01/24	18:20	-86.434	38.1330	4.03	0.16	2
90/01/28	04:59	-102.504	43.3130	4.03	-	1
90/04/07	15:37	-109.519	40.0820	3.59	-	1
90/08/17	21:01	-83.340	36.7940	3.66	0.16	2
90/08/29	19:34	-89.660	35.8300	3.69	-	1
90/09/26	13:18	-89.577	37.1650	4.61	0.02	2
90/10/07	08:47	-75.190	46.3200	3.67	-	1
90/10/19	07:01	-75.590	46.4700	4.87	-	1
90/11/09	03:39	-89.620	36.5400	3.50	-	1
90/12/12	05:15	-66.600	47.0000	3.78	-	1
90/12/20	14:04	-86.671	39.5700	3.60	-	1
90/12/31	03:53	-72.556	47.5790	4.22	-	1
91/01/26	21:49	-111.429	37.6810	3.27	-	1
91/03/06	05:26	-76.874	46.2820	3.71	0.01	2
91/03/15	06:54	-77.916	37.7460	3.95	-	1
91/03/21	04:10	-66.594	49.6980	3.96	0.04	2
91/04/22	01:01	-80.207	37.9410	3.65	-	1
91/05/04	01:18	-89.823	36.5640	4.52	0.05	2
91/06/16	16:46	-76.700	47.0000	3.72	0.06	2
91/06/17	08:53	-74.678	42.6300	4.00	-	1

Table 2. Network-averaged coda m_{bLg} 's for the earthquakes examined, along with event information. The coda- m_{bLg} standard deviations (σ) are provided along with the number of observations (n).

Table 2 (cont.): Network-averaged coda m_{bLg}						
Date	Hr:Min	Longitude	Latitude	m_{bLg}	σ	n
91/07/05	01:47	-73.896	45.2320	3.38	0.12	2
91/07/07	21:24	-91.643	36.6580	4.18	-	1
91/07/20	23:38	-98.042	28.9080	3.53	-	1
91/08/07	12:49	-108.861	43.5020	3.30	-	1
91/08/26	11:49	-100.533	42.1620	3.53	-	1
91/11/11	09:20	-87.894	38.7130	3.63	-	1
91/12/08	03:00	-69.800	47.7000	4.07	0.05	2
92/03/15	06:13	-81.245	41.9110	3.76	0.22	2
92/05/19	05:59	-74.964	46.4440	3.49	-	1
92/08/21	16:31	-80.116	33.0500	4.00	-	1
92/08/31	01:40	-107.041	43.8250	3.48	-	1
92/10/06	15:38	-71.578	43.3240	3.22	-	1
92/11/17	03:58	-74.862	45.7640	3.94	0.06	2
92/12/17	07:18	-97.581	34.7440	3.87	-	1
93/01/08	13:01	-90.030	35.8300	3.64	0.23	2
93/02/06	02:09	-89.730	36.6600	3.47	-	1
93/02/20	13:08	-101.461	42.8300	3.68	-	1
93/02/24	23:52	-105.287	43.7120	4.00	-	1
93/02/25	03:44	-106.062	44.9320	3.50	-	1
93/04/09	12:29	-98.124	28.8110	4.34	-	1
93/04/28	22:40	-89.440	36.1900	3.67	-	1
93/05/06	01:23	-75.500	46.3000	3.35	0.06	2
93/06/01	21:33	-107.575	42.3040	3.75	-	1
93/06/05	01:24	-96.293	45.6740	4.17	0.06	2
93/07/16	10:54	-88.341	31.7470	3.58	-	1
93/07/23	06:30	-105.703	42.4780	3.64	-	1
93/07/30	22:30	-74.120	45.2600	3.56	0.10	2
93/08/30	05:15	-75.050	46.4570	3.44	0.04	2
93/09/23	06:45	-74.605	46.0650	3.63	0.03	2
93/10/10	04:17	-105.868	42.4210	3.78	-	1
93/10/16	06:30	-81.012	41.6980	3.62	0.01	2
93/11/16	07:26	-107.384	43.8840	3.29	-	1
93/11/16	09:31	-73.495	45.1820	4.09	0.01	2
93/12/01	12:47	-70.060	47.5300	3.55	-	1
93/12/13	14:51	-105.499	42.3330	3.78	-	1
93/12/25	16:44	-75.606	46.5060	3.98	0.08	2
93/12/30	23:01	-70.367	47.4530	4.03	-	1
94/01/16	01:49	-76.037	40.3300	4.55	-	2
94/02/03	09:05	-110.976	42.762	5.55	0.05	3
94/02/05	14:55	-89.180	37.3700	4.24	0.11	2
94/03/12	10:43	-77.876	42.7820	3.90	0.11	2
94/03/28	16:28	-65.740	48.9900	3.68	-	1

Table 2 (continued). Network-averaged coda m_{bLg} 's for the earthquakes examined, along with event information. The coda- m_{bLg} standard deviations (σ) are provided along with the number of observations (n).

Table 2 (cont.): Network-averaged Coda m_{bLg}						
Date	Hr:Min	Longitude	Latitude	m_{bLg}	σ	n
94/07/14	12:41	-66.600	47.0000	4.05	0.13	2
94/08/06	19:54	-76.751	35.0670	3.62	-	1
94/08/20	10:45	-91.058	36.1360	3.31	-	1
94/09/02	21:23	-84.604	42.7980	3.69	0.13	2
94/09/16	04:22	-68.223	45.3060	3.62	0.09	2
94/09/25	00:53	-69.960	47.7700	4.04	0.17	2
94/09/26	14:23	-88.935	36.9290	3.62	0.12	2
94/10/02	11:27	-72.277	42.3470	3.67	0.12	2
95/01/18	15:51	-97.596	34.7740	4.18	0.18	2
95/02/15	15:53	-75.040	45.9000	3.46	0.05	3
95/02/19	12:57	-83.470	39.1200	3.47	-	1
95/03/11	08:15	-83.150	36.9830	3.87	0.04	2
95/04/14	00:32	-103.3188	30.2885	5.60	0.07	3
95/04/17	13:45	-80.068	32.9470	3.76	0.09	3
95/05/27	19:51	-89.430	36.1700	3.82	0.09	3
95/05/28	15:28	-87.827	33.1910	3.66	0.09	3
95/06/03	22:44	-76.290	47.0200	3.54	0.11	3
95/06/16	12:13	-71.913	44.2870	3.76	0.02	2
95/07/25	19:34	-111.1055	43.017	3.95	-	1
95/10/26	00:37	-83.121	37.053	3.64	-	1
97/10/24	08:35	-87.339	31.118	4.86	0.03	3
97/11/06	02:34	-74.4	46.8	4.68	0.08	3
98/09/25	19:52	-80.388	41.495	5.00	-	1
01/04/21	17:19	-111.095	43.121	5.05	0.10	2
02/04/20	10:50	-73.66	44.51	5.24	0.01	2
02/06/18	17:37	-87.79	37.99	4.70	0.07	2

Table 2 (continued). Network-averaged coda m_{bLg} 's for the earthquakes examined, along with event information. The coda- m_{bLg} standard deviations (σ) are provided along with the number of observations (n).

Table 3a: m_{bLg} and long-period M_W compiled for ENA earthquakes						
Date	Time	Latitude	Longitude	m_{bLg}	M_W	M_W Reference
1925/3/1	2:19	47.80	-69.80	6.6	6.83	Somerville et al., 1979
1935/11/1	6:03	46.90	-79.10	6.2	6.42	Somerville et al., 1979
1939/10/19	11:53	48.00	-69.70	5.6	5.28	Somerville et al., 1979
1940/12/20	7:27	43.90	-71.40	5.5	5.33	Somerville et al., 1979
1962/2/2	6:43	36.5	-89.6	4.3	4.21	Herrmann, 1979
1963/3/3	17:30	36.7	-90.1	4.8	4.64	Herrmann, 1979
1963/9/4	13:32	71.30	-73.00	5.9	6.08	Somerville et al., 1979
1964/5/14	13:52	65	-87	4.4	4.11	Nuttli, 1983
1965/8/14	13:13	37.2	-89.3	3.8	3.58	Herrmann, 1979
1965/10/21	2:04	37.5	-91.0	4.9	4.58	Herrmann, 1979
1966/1/1	13:23	42.8	-78.2	4.6	4.25	Herrmann, 1979
1967/6/4	16:14	33.6	-90.9	4.5	4.27	Herrmann, 1979
1967/4/10	19:00	40	-105	4.3	4.51	Nuttli, 1983
1967/6/13	19:08	42.9	-78.2	4.4	4.06	Herrmann, 1979
1967/7/21	9:14	37.5	-90.4	4.3	4.02	Herrmann, 1979
1967/8/9	13:25	40	-105	4.9	4.82	Nuttli, 1983
1968/11/9	17:01	38.0	-88.5	5.5	5.27	Herrmann, 1979
1969/1/1	23:35	34.8	-92.6	4.4	4.31	Herrmann, 1979
1969/11/20	1:00	37.4	-81.0	4.6	4.52	Herrmann, 1979
1970/11/17	2:13	35.9	-89.9	4.4	4.08	Herrmann, 1979
1970/12/2	11:03	68	-67	4.9	5.08	Nuttli, 1983
1971/10/2	3:19	64.4	-86.5	5.0	4.64	Herrmann, 1979
1972/1/21	14:33	72	-75	4.2	4.59	Nuttli, 1983
1972/9/15	5:22	41.6	-89.4	4.4	4.10	Herrmann, 1979
1973/6/15	1:09	45.3	-70.9	5.0	4.47	Herrmann, 1979
1973/11/30	7:48	35.8	-84.0	4.6	4.06	Herrmann, 1979
1974/2/15	13:33	36.5	-100.7	4.6	4.34	Herrmann, 1979
1974/4/3	23:05	38.6	-88.1	4.7	4.32	Herrmann, 1979
1975/6/13	22:40	36.5	-89.7	4.2	3.72	Herrmann, 1979
1975/7/9	14:54	45.7	-96.0	4.6	4.28	Herrmann, 1979
1976/3/25	0:41	35.6	-90.5	5.0	4.60	Herrmann, 1979
1976/3/25	01:00	35.6	-90.5	4.5	4.21	Herrmann, 1979
1978/2/18	14:48	46	-74	4.1	3.88	Nuttli, 1983
1978/6/16	11:46	33	-101	4.7	4.48	Nuttli, 1983
1979/8/19	22:49	47.67	-69.60	5.0	4.73	Somerville et al., 1979
1980/7/27	18:51	38	-84	5.2	5.02	Somerville et al., 1979
1982/1/9	12:53	46.98	-66.66	5.8	5.35	Somerville et al., 1979
1982/1/9	12:53	47	-67	5.5	5.55	Nuttli, 1983
1983/10/7	10:18	43.94	-74.26	5.2	4.87	Somerville et al., 1979
1988/11/25	23:46	48.12	71.18	5.9	5.81	Zhao + Helmberger, 1993
1994/1/16	1:49	40.44	-76.04	4.6	4.57	Saikia et al., 1998
1994/2/3	9:05	42.762	-110.976	5.6	5.77	USGS/HVD/BRK

Table 3a. m_{bLg} 's and long-period M_W 's for Eastern North American earthquakes, compiled from other studies.

Table 3a (continued): m_{bLg} and long-period M_W compiled for ENA earthquakes						
Date	Time	Latitude	Longitude	m_{bLg}	M_W	M_W Reference
1995/4/14	0:32	30.289	-103.319	5.55	5.60	USGS/Saikia et al., 1998
1996/5/16	15:41	42.587	-111.209	3.95	4.31	BRK
1997/10/24	8:35	31.118	-87.339	4.8	5.13	Saikia et al., 1998
1997/11/6	2:34	46.8	-74.4	4.8	4.48	Saikia et al., 1998
1998/9/25	19:52	41.495	-80.388	4.8	4.51	USGS/Saikia et al., 1998
2001/4/21	17:19	43.121	-111.095	5.4	5.22	HVD/USGS
2002/4/20	10:50	44.51	-73.66	5.2	5.05	LCSN/HVD
2002/6/18	17:37	37.99	-87.79	5.0	4.56	LCSN

Table 3a (continued). m_{bLg} 's and long-period M_W 's for Eastern North American earthquakes, compiled from other studies.

Table 3b: m_{bLg} and Lg-spectra based M_W compiled for ENA earthquakes						
Date	Time	Latitude	Longitude	m_{bLg}	M_W	M_W (Lg spectra) Reference
1962/2/2	6:43	36.6	-89.7	4.3	4.14	Street, Herrmann & Nuttli, 1975
1962/6/1	11:23	36.0	-90.2	3.2	2.88	Street, Herrmann & Nuttli, 1975
1962/7/14	4:23	36.5	-89.9	3.2	3.12	Street, Herrmann & Nuttli, 1975
1962/7/23	6:05	36.1	-89.4	4.2	3.37	Street, Herrmann & Nuttli, 1975
1963/3/3	17:30	36.7	-90.0	4.7	4.53	Street, Herrmann & Nuttli, 1975
1963/3/31	13:31	36.9	-89.0	3.0	2.46	Street, Herrmann & Nuttli, 1975
1963/4/6	8:12	36.5	-89.6	3.1	2.81	Street, Herrmann & Nuttli, 1975
1963/8/3	0:37	37.0	-88.7	4.0	3.60	Street, Herrmann & Nuttli, 1975
1964/1/16	5:09	36.8	89.5	3.0	3.04	Street, Herrmann & Nuttli, 1975
1964/3/17	2:16	36.2	-89.6	3.5	2.78	Street, Herrmann & Nuttli, 1975
1964/5/23	11:25	36.6	-90.0	4.0	3.45	Street, Herrmann & Nuttli, 1975
1964/5/23	15:00	36.6	-90.0	3.5	2.86	Street, Herrmann & Nuttli, 1975
1965/2/11	3:40	36.4	-89.7	3.5	3.09	Street, Herrmann & Nuttli, 1975
1965/3/6	21:08	37.5	-91.1	4.1	3.45	Street, Herrmann & Nuttli, 1975
1965/3/25	12:59	36.4	-89.5	3.7	3.60	Street, Herrmann & Nuttli, 1975
1965/8/14	5:04	37.2	-89.3	2.9	2.85	Street, Herrmann & Nuttli, 1975
1965/8/14	5:46	37.2	-89.3	3.2	2.88	Street, Herrmann & Nuttli, 1975
1965/8/14	5:59	37.2	-89.3	2.5	2.25	Street, Herrmann & Nuttli, 1975
1965/8/14	13:13	37.2	-89.3	3.8	3.43	Street, Herrmann & Nuttli, 1975
1965/8/15	4:19	37.2	-89.3	3.5	2.89	Street, Herrmann & Nuttli, 1975
1965/8/15	6:07	37.2	-89.3	3.4	3.01	Street, Herrmann & Nuttli, 1975
1965/8/15	11:19	37.2	-89.3	2.7	2.26	Street, Herrmann & Nuttli, 1975
1965/10/21	2:04	37.5	-91.1	4.9	4.51	Street, Herrmann & Nuttli, 1975
1965/11/4	7:43	37.1	-91.0	3.8	3.28	Street, Herrmann & Nuttli, 1975
1966/2/12	4:32	35.9	-90.0	3.6	3.26	Street, Herrmann & Nuttli, 1975
1966/2/13	6:29	33.6	-87.0	3.5	3.60	Street, Herrmann & Nuttli, 1975
1966/2/13	23:19	37.0	-91.0	3.2	3.28	Street, Herrmann & Nuttli, 1975
1966/2/14	0:08	37.0	-91.0	3.1	2.84	Street, Herrmann & Nuttli, 1975
1966/2/26	8:10	37.1	-91.0	3.6	3.17	Street, Herrmann & Nuttli, 1975
1966/12/6	8:00	38.8	-92.8	2.9	2.81	Street, Herrmann & Nuttli, 1975
1967/7/21	9:14	37.5	-90.6	4.3	3.91	Street, Herrmann & Nuttli, 1975
1967/8/5	11:37	38.3	-90.6	2.8	2.61	Street, Herrmann & Nuttli, 1975
1968/2/10	1:34	36.5	-89.9	3.5	3.75	Street, Herrmann & Nuttli, 1975
1969/1/1	23:35	34.8	-92.6	4.5	4.32	Street, Herrmann & Nuttli, 1975
1969/2/28	13:10	37.9	-88.9	3.2	2.75	Street, Herrmann & Nuttli, 1975
1970/3/27	3:44	36.5	-89.7	3.5	2.73	Street, Herrmann & Nuttli, 1975
1970/11/17	2:13	35.9	-90.2	4.4	4.00	Street, Herrmann & Nuttli, 1975
1970/11/30	4:46	36.2	-89.9	2.8	2.91	Street, Herrmann & Nuttli, 1975
1971/2/12	12:44	38.5	-87.9	3.3	3.03	Street, Herrmann & Nuttli, 1975
1971/4/13	14:00	35.7	-90.1	2.8	2.66	Street, Herrmann & Nuttli, 1975
1971/10/1	18:49	35.8	-90.4	4.1	3.68	Street, Herrmann & Nuttli, 1975
1971/10/18	6:39	36.7	-89.6	3.0	2.61	Street, Herrmann & Nuttli, 1975

Table 3b. m_{bLg} 's and Lg-spectra based M_W 's for Eastern North American earthquakes, compiled from other studies.

Table 3b (continued): m_{bLg} and Lg-spectra based M_W compiled for ENA earthquakes						
Date	Time	Latitude	Longitude	m_{bLg}	M_W	M_W (Lg spectra) Reference
1972/2/1	5:42	36.4	-90.8	4.2	3.43	Street, Herrmann & Nuttli, 1975
1972/3/29	20:38	36.2	-89.6	3.7	3.48	Street, Herrmann & Nuttli, 1975
1972/5/7	2:12	35.9	-90.6	3.4	3.12	Street, Herrmann & Nuttli, 1975
1972/6/19	5:46	37.0	-89.1	3.2	2.84	Street, Herrmann & Nuttli, 1975
1972/6/21	2:31	37.1	-89.9	2.7	2.26	Street, Herrmann & Nuttli, 1975
1972/9/15	5:22	41.6	-89.3	4.4	4.02	Street, Herrmann & Nuttli, 1975
1973/1/7	22:56	37.4	-87.3	3.2	2.95	Street, Herrmann & Nuttli, 1975
1973/10/3	3:50	35.7	-90.1	3.4	2.98	Street, Herrmann & Nuttli, 1975
1973/10/9	20:15	36.5	-89.6	3.7	3.25	Street, Herrmann & Nuttli, 1975
1974/1/8	1:12	36.2	-89.4	4.0	3.60	Street, Herrmann & Nuttli, 1975
1974/6/5	8:07	36.8	-89.9	3.6	3.13	Street, Herrmann & Nuttli, 1975
1925/3/1	2:19	47.8	-69.8	6.6	6.19	Street & Turcotte, 1977
1929/8/12	11:25	42.9	-78.3	5.2	4.69	Street & Turcotte, 1977
1929/11/18	20:32	44.5	56.3	6.7	6.46	Street & Turcotte, 1977
1935/11/1	6:03	46.8	-79.10	6.2	5.59	Street & Turcotte, 1977
1938/8/23	3:36	40.2	-74.5	3.9	3.53	Street & Turcotte, 1977
1938/8/23	5:04	40.2	-73.7	4.0	3.55	Street & Turcotte, 1977
1938/8/23	7:05	40.2	-74.2	3.7	3.58	Street & Turcotte, 1977
1939/10/19	11:54	47.8	-70.0	5.6	5.10	Street & Turcotte, 1977
1940/1/28	23:12	41.6	-70.8	2.7	2.69	Street & Turcotte, 1977
1940/12/20	7:27	43.8	-71.3	5.5	5.25	Street & Turcotte, 1977
1940/12/24	14:33	43.8	-71.3	2.8	2.75	Street & Turcotte, 1977
1940/12/25	5:04	43.8	-71.3	3.7	3.37	Street & Turcotte, 1977
1940/12/27	19:56	43.8	-71.3	3.8	3.41	Street & Turcotte, 1977
1941/1/21	2:28	43.8	-71.3	2.8	2.75	Street & Turcotte, 1977
1941/1/23	0:15	43.8	-71.3	2.9	2.61	Street & Turcotte, 1977
1943/1/14	21:32	45.2	-69.6	4.3	3.93	Street & Turcotte, 1977
1944/9/5	4:39	44.9	-74.8	5.8	5.52	Street & Turcotte, 1977
1949/10/5	2:34	44.8	-70.5	4.4	4.17	Street & Turcotte, 1977
1951/9/3	21:26	41.1	-74.3	3.8	3.37	Street & Turcotte, 1977
1952/10/14	22:04	48.0	-69.8	4.9	4.02	Street & Turcotte, 1977
1957/4/26	11:40	43.6	-69.8	4.7	4.35	Street & Turcotte, 1977
1963/10/16	15:31	42.4	-70.7	3.9	3.39	Street & Turcotte, 1977
1963/10/23	20:05	42.6	-70.0	2.4	2.37	Street & Turcotte, 1977
1963/10/30	22:37	42.7	-70.8	2.4	2.58	Street & Turcotte, 1977
1967/7/1	14:10	44.9	-69.9	2.9	2.69	Street & Turcotte, 1977
1967/7/1	16:07	44.4	-69.9	3.4	3.28	Street & Turcotte, 1977
1974/6/7	19:45	41.6	-73.9	2.8	2.85	Street & Turcotte, 1977
1975/6/9	18:39	44.9	-73.6	3.5	3.28	Street & Turcotte, 1977
1975/10/6	22:21	44.6	-56.5	4.8	4.04	Street & Turcotte, 1977
1975/11/3	20:54	43.9	-74.6	4.0	3.68	Street & Turcotte, 1977
1976/3/11	3:30	41.6	-71.3	2.2	2.06	Street & Turcotte, 1977

Table 3b (continued). m_{bLg} 's and Lg-spectra based M_W 's for Eastern North American earthquakes, compiled from other studies.

Table 3b (continued): m_{bLg} and Lg-spectra based M_W compiled for ENA earthquakes						
Date	Time	Latitude	Longitude	m_{bLg}	M_W	M_W (Lg spectra) Reference
1982/1/9	12:53	46.984	-66.678	5.8	5.45	Street '84
1982/1/9	16:36	47.023	-66.648	5.0	4.10	Street '84
1982/1/11	21:41	46.950	-66.659	5.4	4.78	Street '84
1982/3/31	21:02	47.00	-66.60	4.5	4.14	Street '84
1982/6/16	11:43	46.970	-66.990	4.3	3.83	Street '84
1982/1/19	4:39	35.193	-92.254	3.4	3.08	Street '84
1982/1/20	14:01	35.200	-92.210	3.5	3.07	Street '84
1982/1/21	0:33	35.176	-92.211	4.2	3.86	Street '84
1982/1/21	0:37	35.162	-92.241	4.5	3.77	Street '84
1982/1/21	15:45	35.193	-92.202	3.5	3.13	Street '84
1982/1/22	23:54	35.217	-92.210	3.9	3.33	Street '84
1982/1/24	3:22	35.198	-92.220	4.2	3.58	Street '84
1982/2/1	5:55	35.184	-92.227	3.1	2.69	Street '84
1982/2/1	7:25	35.189	-92.221	3.0	2.80	Street '84
1982/2/24	19:27	35.199	-92.236	3.6	3.05	Street '84
1982/3/1	0:12	35.187	-92.215	3.8	3.30	Street '84
1982/5/31	18:21	35.195	-92.230	3.4	3.05	Street '84
1982/6/30	16:21	35.190	-92.225	3.2	2.71	Street '84
1982/7/5	4:13	35.184	-92.229	3.6	3.23	Street '84
1980/3/11	4:15	46.79	-71.86	3.7	3.37	Boatwright '94
1980/4/3	16:57	48.77	-67.94	4.0	3.56	Boatwright '94
1981/6/16	17:55	47.47	-70.00	3.7	3.11	Boatwright '94
1981/7/4	23:16	45.14	-74.62	3.7	3.17	Boatwright '94
1981/7/13	4:48	49.91	-66.92	3.7	3.25	Boatwright '94
1981/9/18	7:16	46.05	-75.05	3.5	2.97	Boatwright '94
1981/9/30	23:41	46.32	-75.59	3.5	2.90	Boatwright '94
1981/10/28	19:56	49.84	-65.25	3.9	3.41	Boatwright '94
1981/11/28	5:12	46.94	-66.76	3.7	3.35	Boatwright '94
1982/1/9	17:27	47.00	-66.60	3.8	3.33	Boatwright '94
1982/1/9	22:45	47.00	-66.60	3.7	3.28	Boatwright '94
1982/1/11	21:41	47.00	-66.60	5.4	5.17	Boatwright '94
1982/1/13	17:56	47.00	-66.60	4.0	3.16	Boatwright '94
1982/1/15	12:37	47.00	-66.60	3.8	3.39	Boatwright '94
1982/1/17	13:33	47.00	-66.60	3.6	3.21	Boatwright '94
1982/1/19	0:14	43.51	-71.62	4.5	3.97	Boatwright '94
1982/3/16	11:14	47.00	-66.60	3.5	3.20	Boatwright '94
1982/3/31	21:02	47.00	-66.60	5.0	3.92	Boatwright '94
1982/4/2	13:50	47.00	-66.60	4.3	3.64	Boatwright '94
1982/4/11	18:00	47.00	-66.60	4.0	3.48	Boatwright '94
1982/4/18	22:47	47.00	-66.60	4.1	3.46	Boatwright '94
1982/5/6	16:28	47.00	-66.60	4.0	3.43	Boatwright '94
1982/6/16	11:43	47.01	-66.95	4.7	3.91	Boatwright '94

Table 3b (continued). m_{bLg} 's and Lg-spectra based M_W 's for Eastern North American earthquakes, compiled from other studies.

Table 3b (continued): m_{bLg} and Lg-spectra based M_W compiled for ENA earthquakes						
Date	Time	Latitude	Longitude	m_{bLg}	M_W	M_W (Lg spectra) Reference
1982/6/23	0:22	47.37	-77.06	3.5	2.84	Boatwright '94
1982/7/13	2:18	46.04	-74.55	3.8	3.20	Boatwright '94
1982/7/28	5:35	47.00	-66.60	3.7	3.28	Boatwright '94
1982/8/6	6:29	45.89	-75.46	3.7	3.06	Boatwright '94
1982/8/13	1:06	46.67	-78.53	4.3	3.54	Boatwright '94
1982/9/3	23:14	45.68	-76.58	3.7	3.15	Boatwright '94
1982/10/26	15:31	47.00	-66.60	3.5	3.07	Boatwright '94
1982/12/4	16:08	47.54	-70.22	3.9	3.30	Boatwright '94
1983/1/17	19:35	49.09	-67.07	4.1	3.56	Boatwright '94
1983/5/13	17:26	47.00	-66.60	3.5	3.08	Boatwright '94
1983/5/13	23:40	47.00	-66.60	3.9	3.62	Boatwright '94
1983/5/16	2:01	47.69	-69.89	3.8	3.37	Boatwright '94
1983/5/29	5:45	44.48	-70.42	4.1	3.68	Boatwright '94
1983/8/12	14:08	44.96	-67.72	3.5	2.95	Boatwright '94
1983/10/7	10:18	43.94	-74.25	5.6	4.99	Boatwright '94
1983/10/7	10:39	43.95	-74.25	3.6	3.17	Boatwright '94
1983/10/11	4:10	45.20	-75.75	4.1	3.50	Boatwright '94
1983/11/17	22:58	47.00	-66.60	3.7	3.25	Boatwright '94
1983/12/28	12:24	47.07	-76.28	3.5	2.84	Boatwright '94
1984/2/24	3:17	47.00	-66.60	3.7	3.26	Boatwright '94
1984/4/11	19:07	49.30	-67.52	3.8	3.37	Boatwright '94
1984/9/23	8:56	45.97	-64.81	3.6	3.26	Boatwright '94
1984/11/30	5:54	47.00	-66.60	3.8	3.30	Boatwright '94
1985/3/3	12:15	47.39	-70.47	3.1	2.73	Boatwright '94
1985/4/12	5:27	45.37	-70.68	3.5	2.90	Boatwright '94
1985/10/5	5:34	47.00	-66.60	4.0	3.43	Boatwright '94
1985/10/19	10:07	41.21	-73.98	4.1	3.54	Boatwright '94
1986/1/11	13:30	47.70	-70.12	4.0	3.33	Boatwright '94
1986/1/31	16:46	41.70	-81.18	5.0	4.61	Boatwright '94
1986/7/12	8:19	40.54	-84.35	4.5	4.27	Boatwright '94
1986/8/6	11:19	46.37	-75.22	3.5	3.10	Boatwright '94
1986/8/18	12:28	47.53	-70.02	3.0	2.60	Boatwright '94
1986/9/19	15:53	47.30	-70.32	4.2	3.55	Boatwright '94
1986/10/25	17:16	43.42	-71.56	3.9	3.80	Boatwright '94
1986/11/9	19:57	49.24	-67.41	4.2	3.66	Boatwright '94
1987/3/18	19:44	47.72	-70.19	3.3	2.73	Boatwright '94
1987/7/13	5:49	41.93	-80.71	4.1	3.58	Boatwright '94
1987/8/6	9:32	47.43	-70.28	3.4	2.87	Boatwright '94
1987/9/26	17:44	44.49	-74.52	3.8	3.26	Boatwright '94
1987/10/23	12:31	45.76	-74.51	3.7	3.12	Boatwright '94
1987/11/11	7:58	45.77	-75.34	3.5	2.97	Boatwright '94
1987/11/11	8:00	45.78	-75.34	3.5	2.96	Boatwright '94

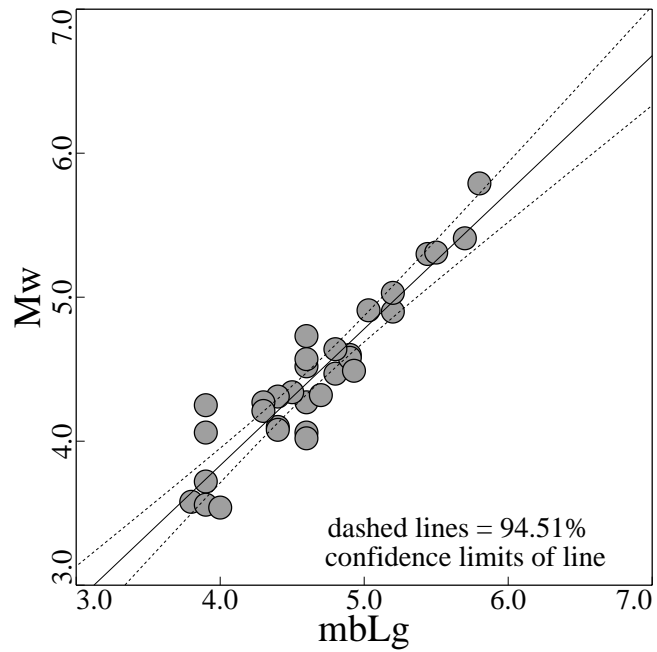
Table 3b (continued). m_{bLg} 's and Lg-spectra based M_W 's for Eastern North American earthquakes, compiled from other studies.

Table 3b (continued): m_{bLg} and Lg-spectra based M_W compiled for ENA earthquakes						
Date	Time	Latitude	Longitude	m_{bLg}	M_W	M_W (Lg spectra) Reference
1988/1/2	9:25	47.42	-70.43	3.6	3.06	Boatwright '94
1988/1/24	4:33	47.44	-70.46	3.1	2.66	Boatwright '94
1988/1/28	8:38	48.00	-65.66	3.8	3.51	Boatwright '94
1988/3/10	14:42	46.34	-75.67	3.7	3.21	Boatwright '94
1988/3/13	16:24	47.44	-70.38	3.1	2.74	Boatwright '94
1988/4/24	1:14	46.01	-64.92	3.7	3.19	Boatwright '94
1988/5/9	1:23	47.00	-66.60	3.5	3.06	Boatwright '94
1988/5/15	6:10	45.16	-75.61	3.3	2.90	Boatwright '94
1988/8/9	13:57	45.01	-74.99	3.4	2.76	Boatwright '94
1988/8/26	5:59	47.00	-66.60	3.8	3.43	Boatwright '94
1988/10/20	13:09	44.56	-71.17	3.8	3.41	Boatwright '94
1988/11/23	9:11	48.13	-71.20	4.6	4.04	Boatwright '94
1988/11/25	23:46	48.12	-71.18	6.5	5.81	Boatwright '94
1988/11/26	3:38	48.14	-71.30	4.1	3.46	Boatwright '94
1989/1/19	21:36	48.06	-71.01	3.6	3.19	Boatwright '94
1989/1/31	14:39	47.44	-70.67	3.1	2.81	Boatwright '94
1989/2/10	1:04	50.07	-64.65	4.3	3.76	Boatwright '94
1989/3/9	9:41	47.72	-69.86	4.3	3.72	Boatwright '94
1989/3/16	4:17	60.06	-70.06	5.6	4.81	Boatwright '94
1989/8/10	21:17	46.66	-65.79	3.5	3.20	Boatwright '94
1989/10/13	14:04	47.39	-70.13	3.2	2.96	Boatwright '94
1989/11/4	4:50	46.22	-75.72	3.4	2.89	Boatwright '94
1989/11/16	9:24	46.58	-76.60	4.0	3.54	Boatwright '94
1989/11/22	23:02	47.46	-70.34	3.4	2.97	Boatwright '94
1990/3/3	2:06	47.86	-69.98	3.6	3.41	Boatwright '94
1990/3/13	19:10	47.53	-70.14	3.2	2.79	Boatwright '94
1990/4/21	1:23	47.55	-70.07	3.1	2.82	Boatwright '94
1990/4/23	0:28	47.41	-70.18	3.0	2.64	Boatwright '94
1990/10/7	8:47	46.31	-75.19	3.9	3.56	Boatwright '94
1990/10/19	7:01	46.47	-75.59	5.1	4.49	Boatwright '94
1990/10/21	13:38	47.40	-70.36	3.3	2.92	Boatwright '94
1990/12/18	7:10	47.26	-70.34	3.3	2.99	Boatwright '94

Table 3b (continued). m_{bLg} 's and Lg-spectra based M_W 's for Eastern North American earthquakes, compiled from other studies.

M_w vs. mbLg(CEUS):

(a)

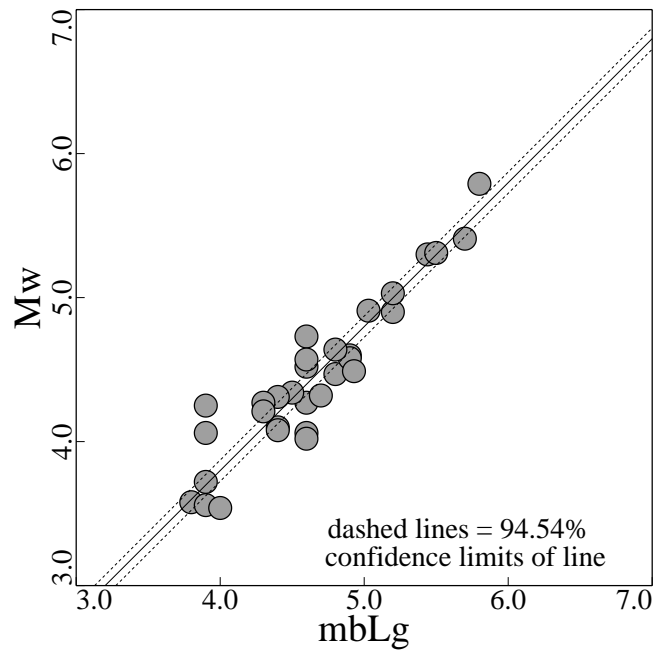


$$M_w = (0.949 \pm 0.139) \times mbLg + 0.037 \pm 0.073$$

(cor. coef.=0.979, std. error of est.=0.20, ndata=31)

M_w vs. mbLg(CEUS):

(b)



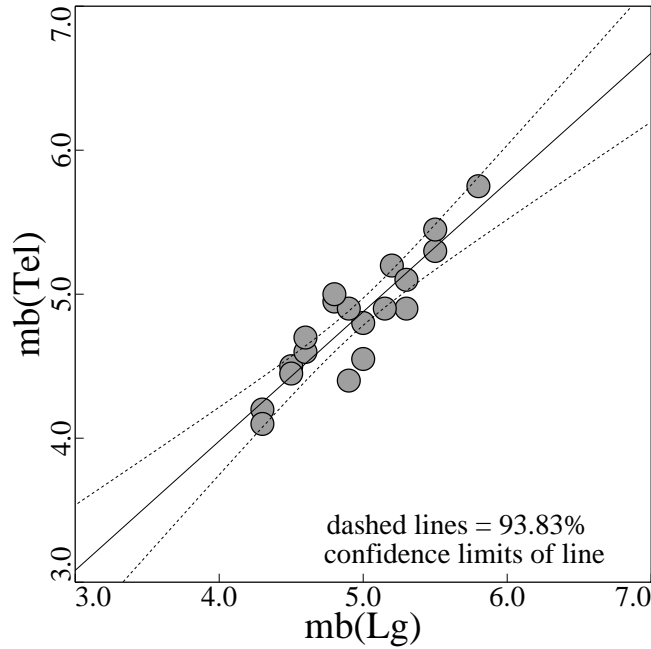
$$M_w = 1.000 \times mbLg - 0.202 \pm 0.073$$

(cor. coef.=0.979, std. error of est.=0.20, ndata=31)

Figure 1. M_w vs. m_b scaling relationship for earthquakes from the USGS NEHRP catalog: (a) unconstrained (free-slope) regression, (b) constrained (fixed-slope, m = 1) result.

mb(Tel) vs. mb(Lg): ENA

(a)

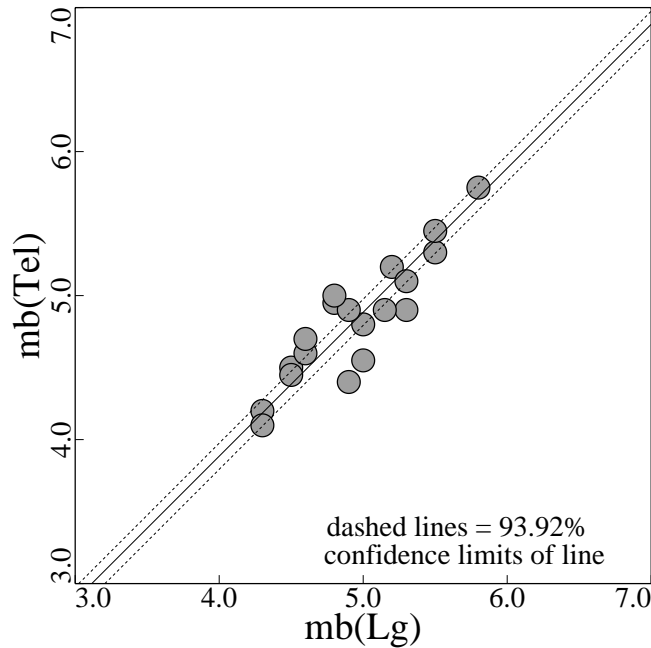


$$mb(Tel) = (0.898 \pm 0.216) \times mb(Lg) + 0.389 \pm 0.089$$

(cor. coef.=0.981, std. error of est.=0.19, ndata=19)

mb(Tel) vs. mb(Lg): ENA

(b)



$$mb(Tel) = 1.000 \times mb(Lg) - 0.116 \pm 0.089$$

(cor. coef.=0.981, std. error of est.=0.19, ndata=19)

Figure 2. Teleseismic m_b vs. regional m_{bLg} scaling relationship for a set of eastern North American earthquakes: (a) unconstrained (free slope) regression, (b) constrained (fixed-slope, $m = 1$) result.

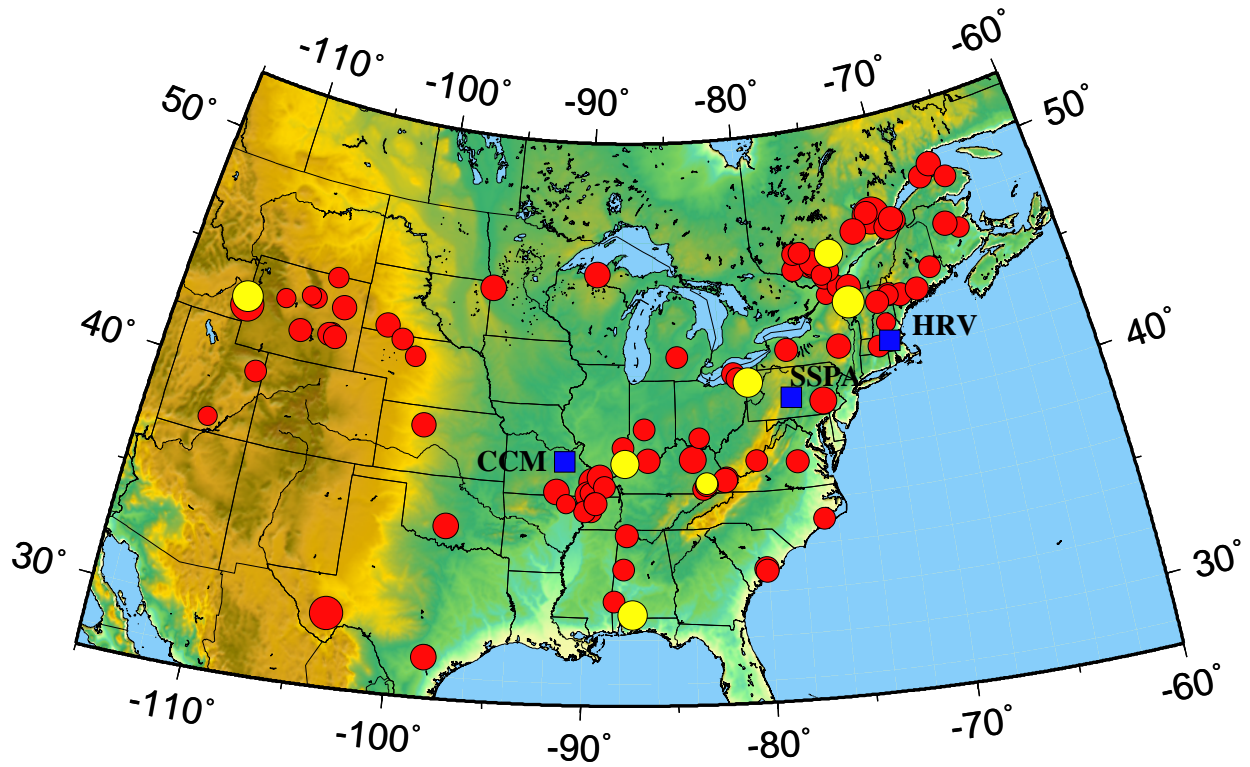


Figure 3. Map of study area, showing stations (blue squares), CEUS catalog earthquakes (red circles) and post-CEUS catalog events (yellow circles).

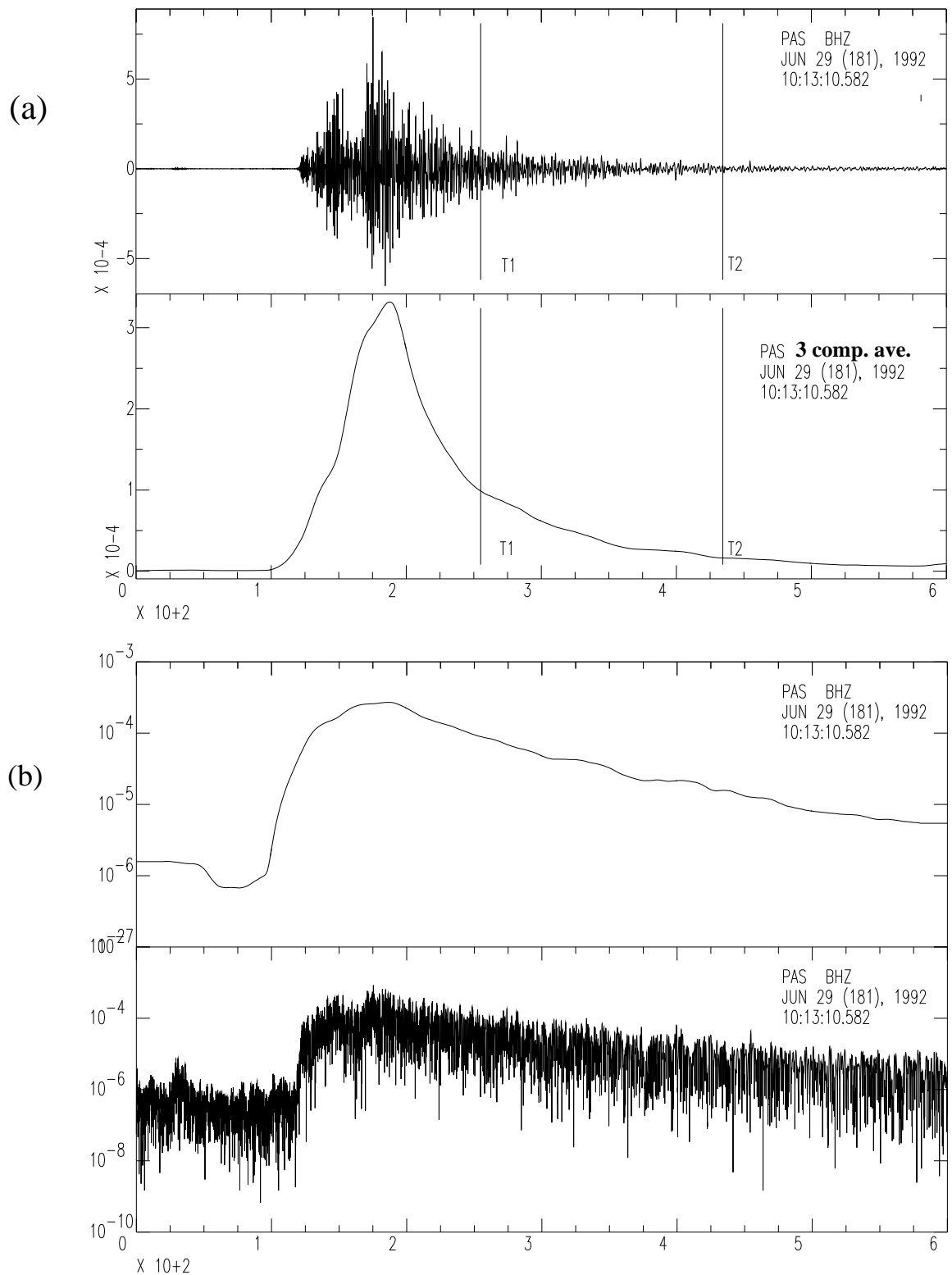


Figure 4. (a) Example WWSP-convolved displacement waveform (top) and the corresponding smoothed envelope of the three components (bottom); T1 and T2 denote the portion of the time window of the time series over which the coda amplitude and duration are measured. (b) Comparison of log amplitude of the envelope (top) to that of the displacement (bottom) for the same single-component record

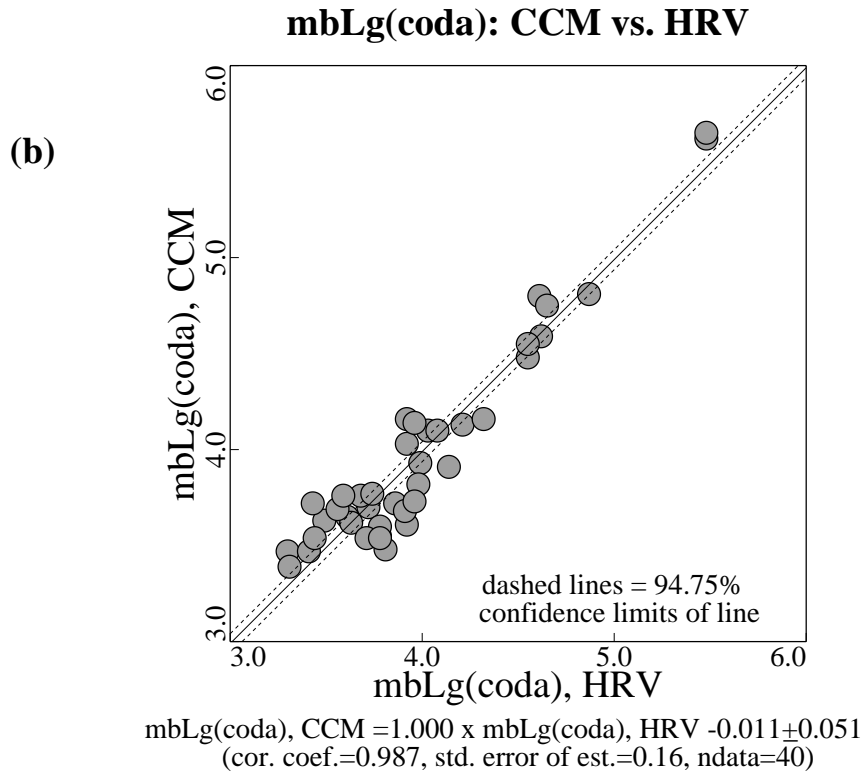
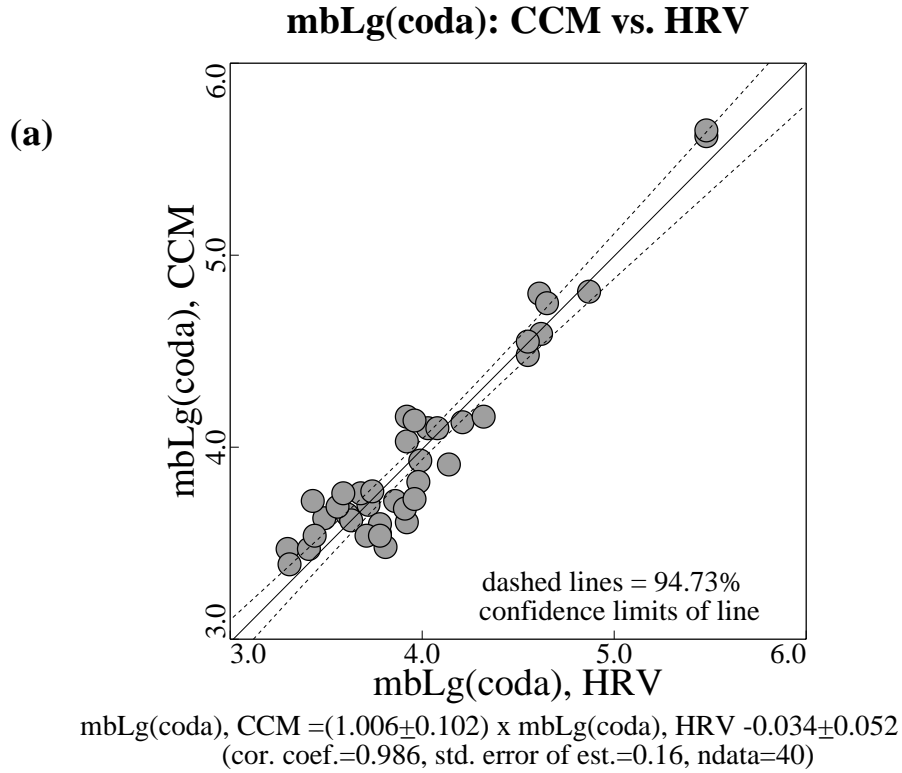


Figure 5. Inter-station $m_{bLg}(coda)$ comparison for CCM and HRV: (a) unconstrained (free-slope) regression, (b) constrained (fixed-slope, $m = 1$) result.

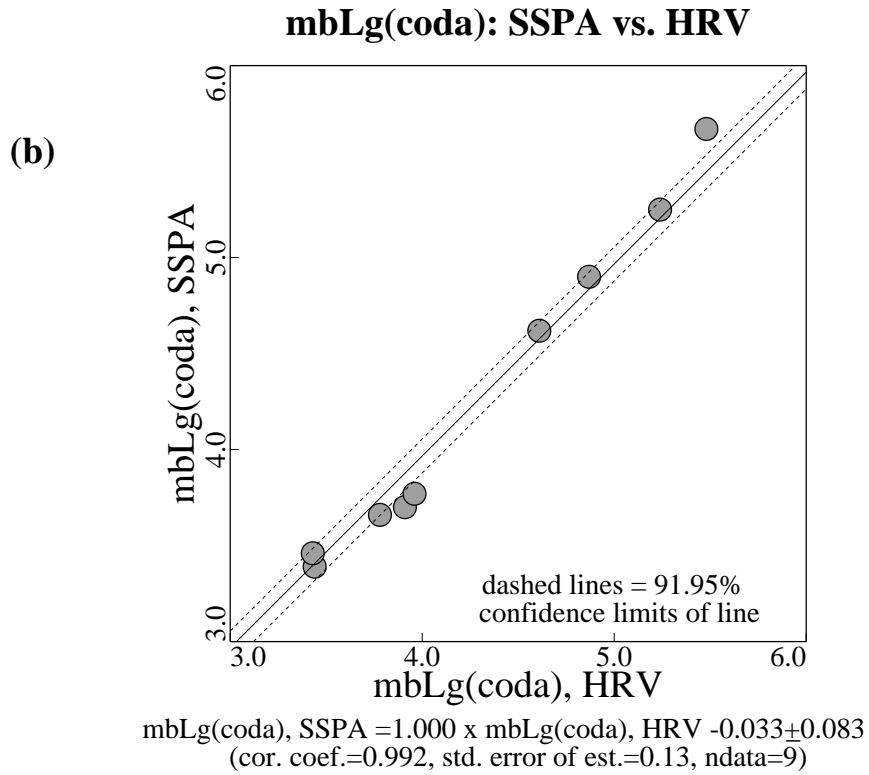
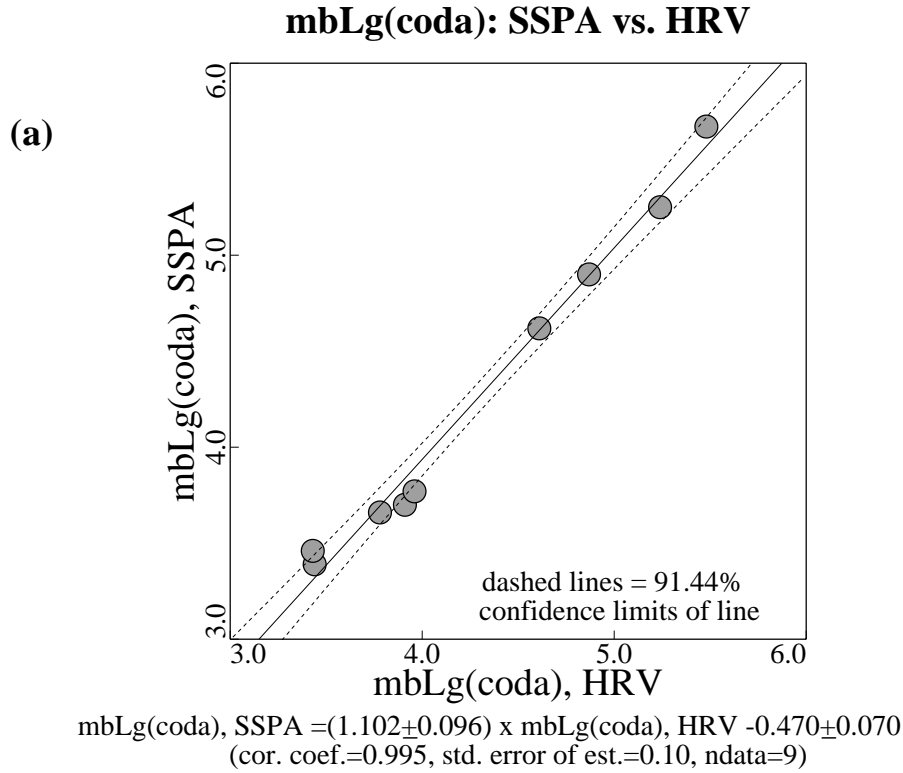


Figure 6. Inter-station $m_{bLg}(coda)$ comparison for SSPA and HRV: (a) unconstrained (free-slope) regression, (b) constrained (fixed-slope, $m = 1$) result.

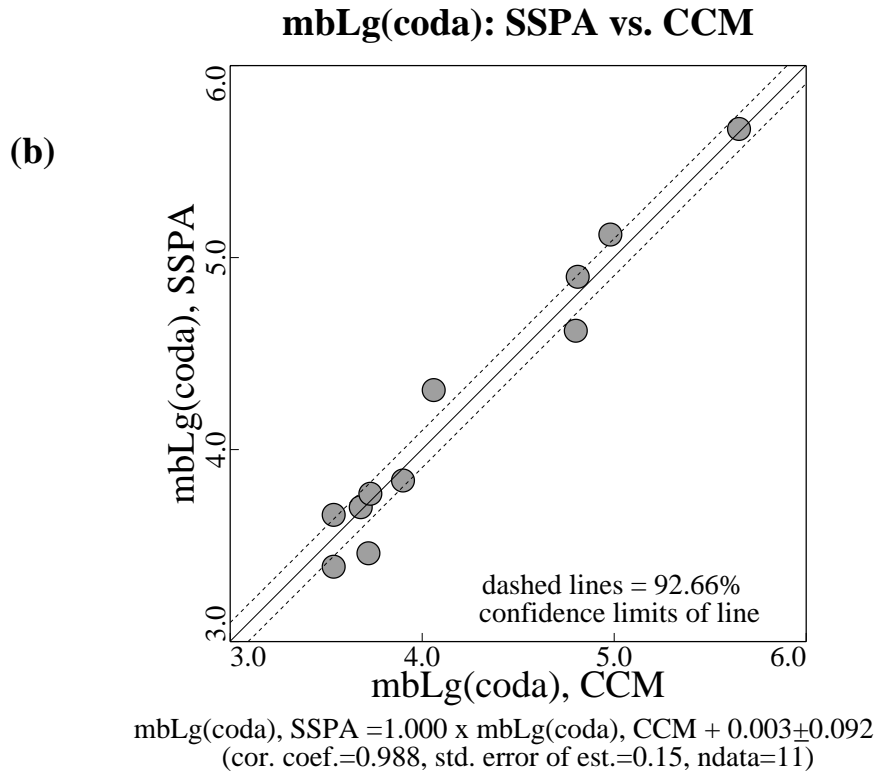
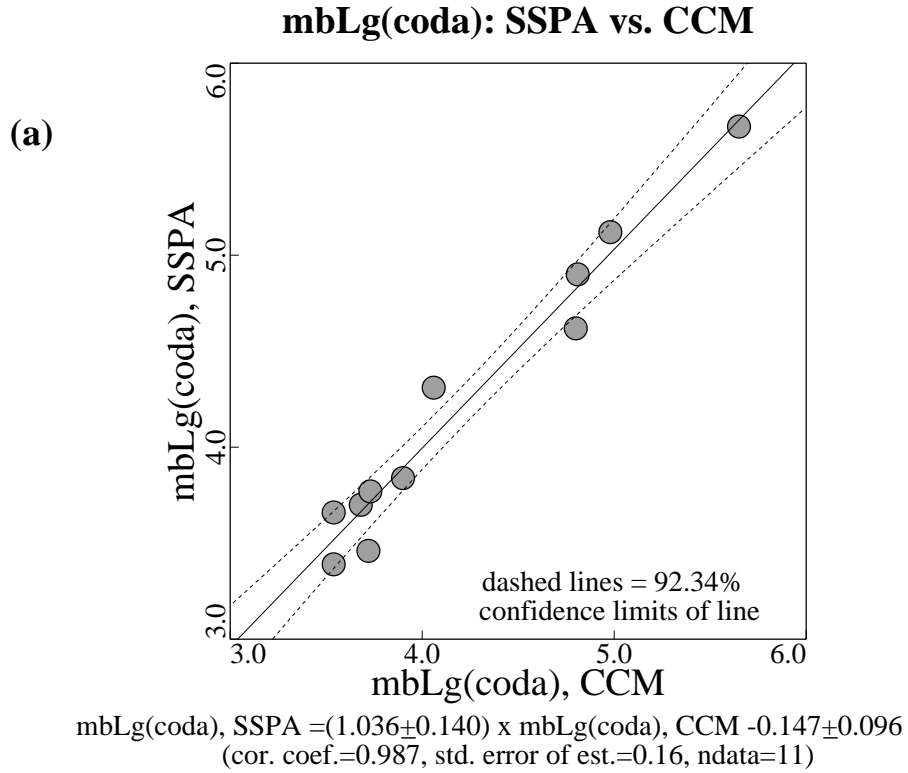


Figure 7. Inter-station $m_{bLg}(coda)$ comparison for SSPA and CCM: (a) unconstrained (free-slope) regression, (b) constrained (fixed-slope, $m = 1$) result.

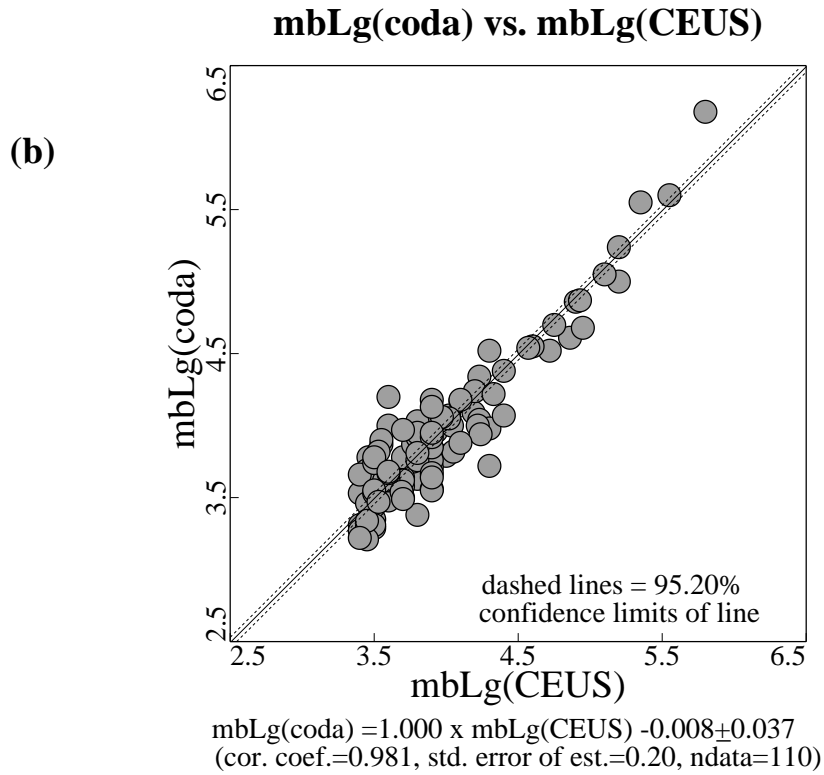
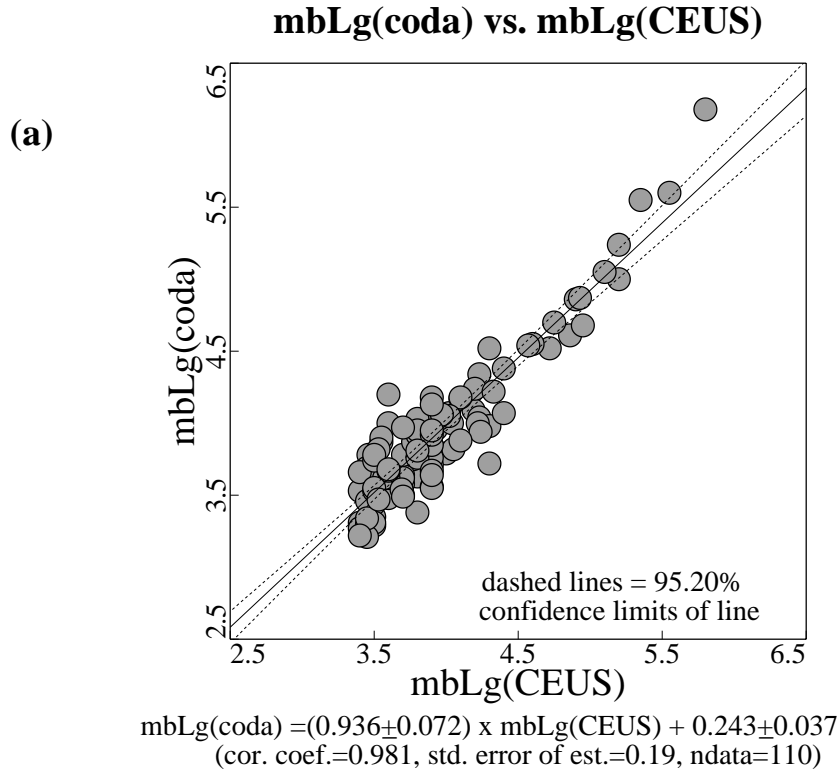
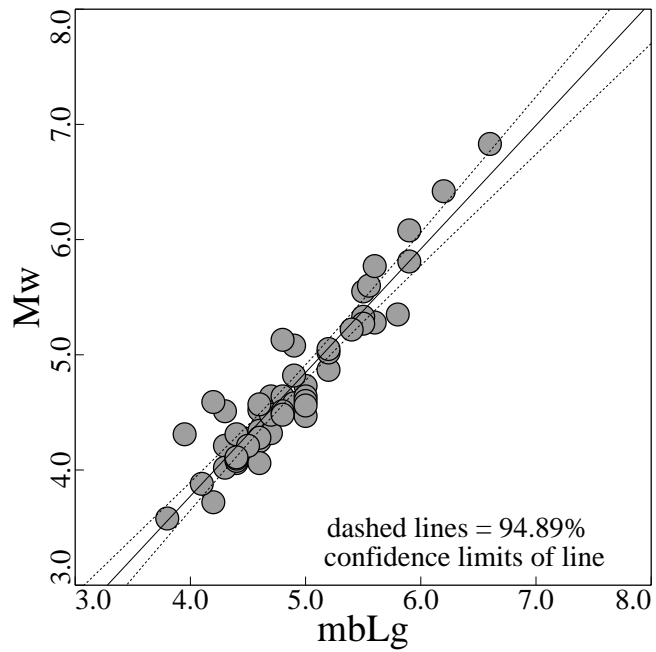


Figure 8. Network-averaged coda m_{bLg} vs. CEUS catalog m_{bLg} : (a) unconstrained (free-slope) regression, (b) constrained (fixed-slope, $m = 1$) result.

Mw vs. mbLg: ENA

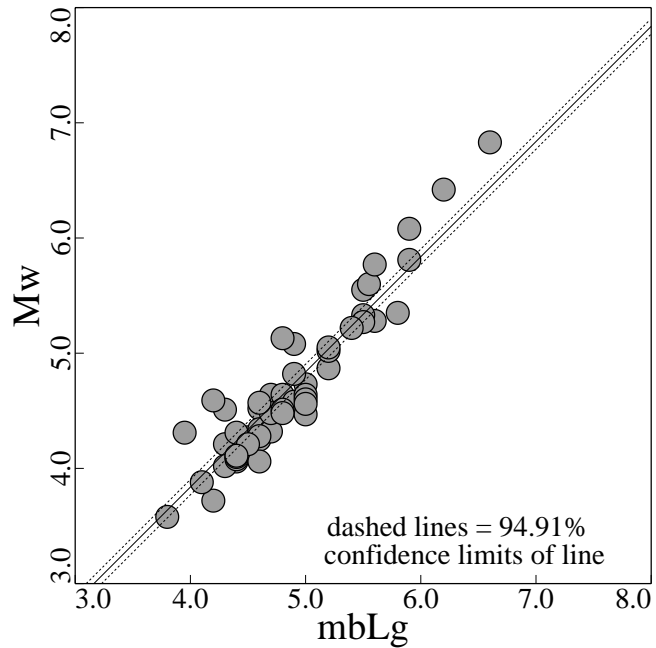
(a)



$M_w = (1.073 \pm 0.112) \times m_{bLg} - 0.518 \pm 0.066$
(cor. coef.=0.972, std. error of est.=0.23, ndata=51)

Mw vs. mbLg: ENA

(b)

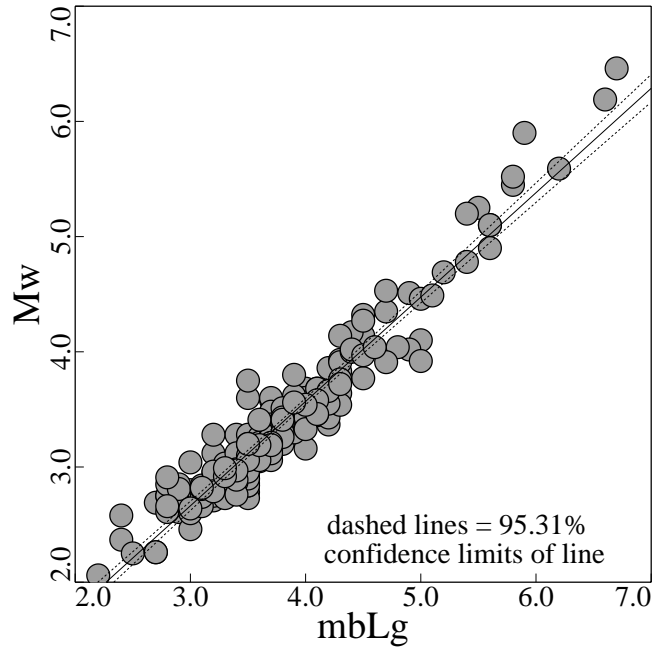


$M_w = 1.000 \times m_{bLg} - 0.163 \pm 0.066$
(cor. coef.=0.972, std. error of est.=0.24, ndata=51)

Figure 9. M_w (long-period) vs. m_{bLg} scaling relationship for earthquakes in eastern North America: (a) unconstrained (free-slope) regression, (b) constrained (fixed-slope, $m = 1$) result.

M_w(Lg spectra) vs. mbLg: ENA

(a)

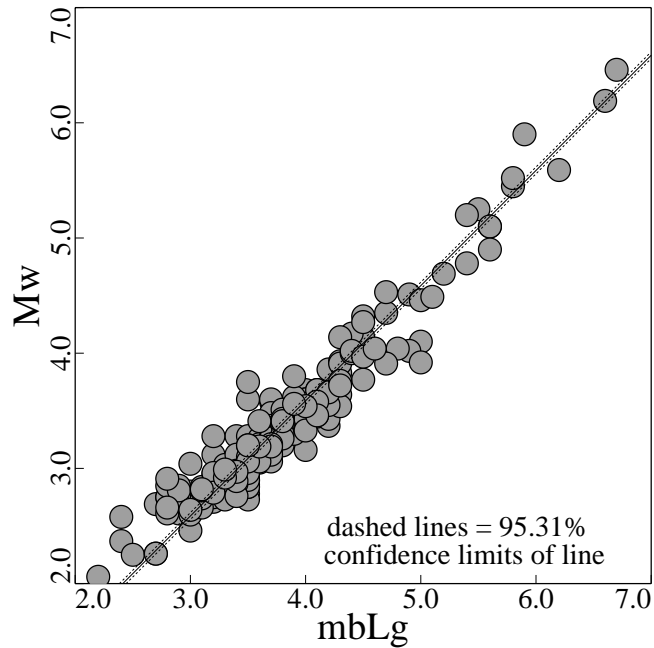


$$M_w = (0.906 \pm 0.036) \times m_bL_g - 0.056 \pm 0.027$$

(cor. coef.=0.981, std. error of est.=0.19, ndata=201)

M_w(Lg spectra) vs. mbLg: ENA

(b)



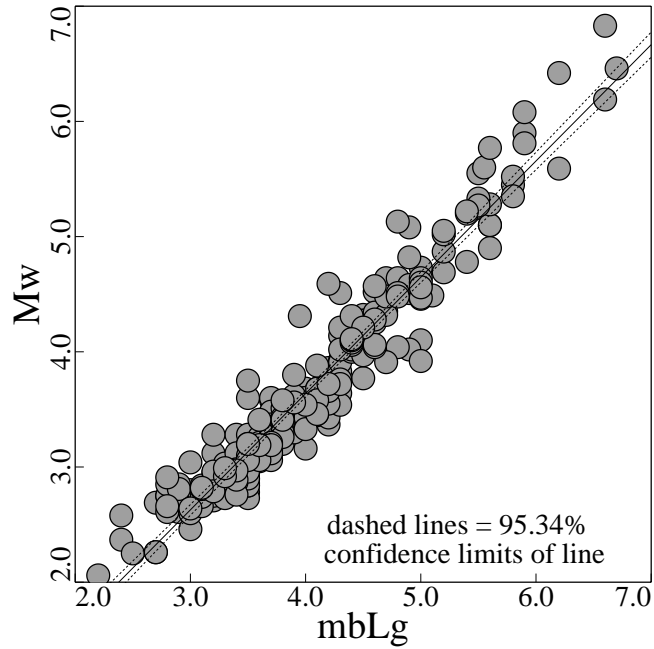
$$M_w = 1.000 \times m_bL_g - 0.413 \pm 0.029$$

(cor. coef.=0.979, std. error of est.=0.21, ndata=201)

Figure 10. M_w (Lg-spectra) vs. m_bL_g scaling relationship for earthquakes in eastern North America: (a) unconstrained (free-slope) regression, (b) constrained (fixed-slope, $m = 1$) result.

M_w(all) vs. m_bL_g: ENA

(a)

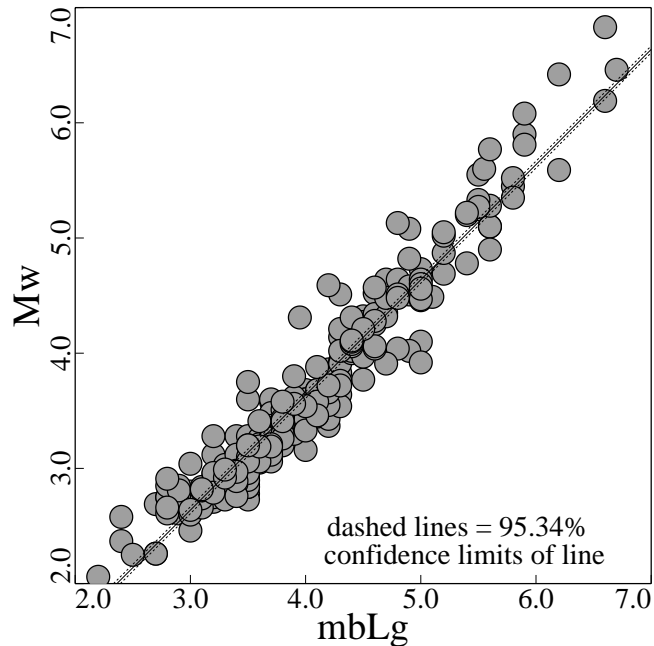


$$M_w = (1.010 \pm 0.035) \times m_b L_g - 0.402 \pm 0.030$$

(cor. coef.=0.972, std. error of est.=0.23, n_{data}=252)

M_w(all) vs. m_bL_g: ENA

(b)



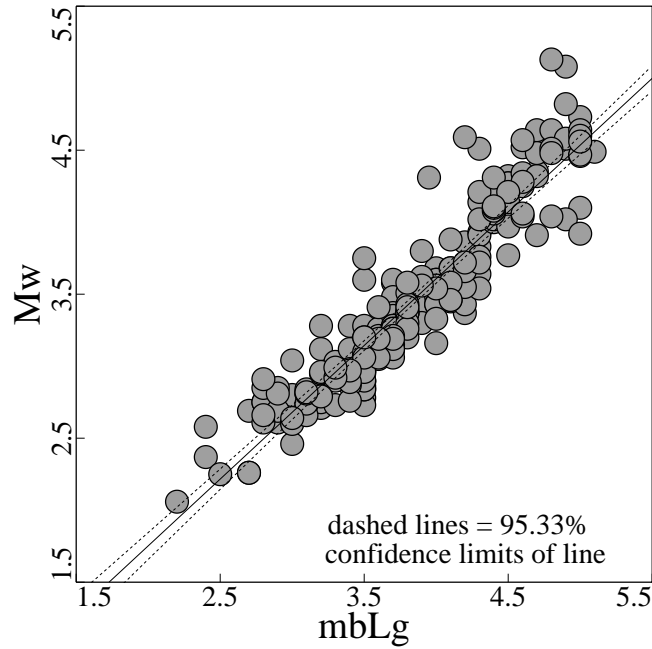
$$M_w = 1.000 \times m_b L_g - 0.363 \pm 0.029$$

(cor. coef.=0.972, std. error of est.=0.23, n_{data}=252)

Figure 11. M_w (both long-period and L_g-spectra) vs. $m_b L_g$ scaling relationship for earthquakes in eastern North America: (a) unconstrained (free-slope) regression, (b) constrained (fixed-slope, $m = 1$) result.

M_w vs. mbL_g: ENA (mbL_g < 5.1)

(a)

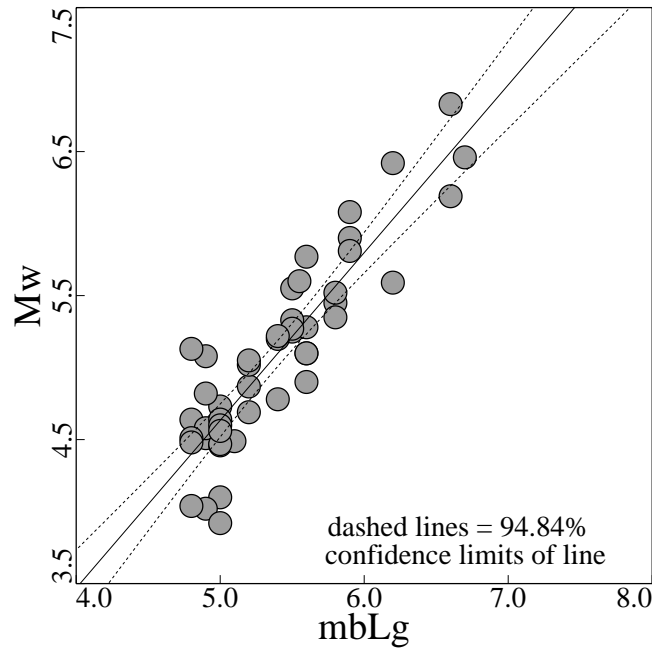


$$M_w = (0.928 \pm 0.049) \times m_{bL_g} - 0.104 \pm 0.030$$

(cor. coef.=0.975, std. error of est.=0.22, ndata=224)

M_w vs. mbL_g: ENA (mbL_g > 4.75)

(b)



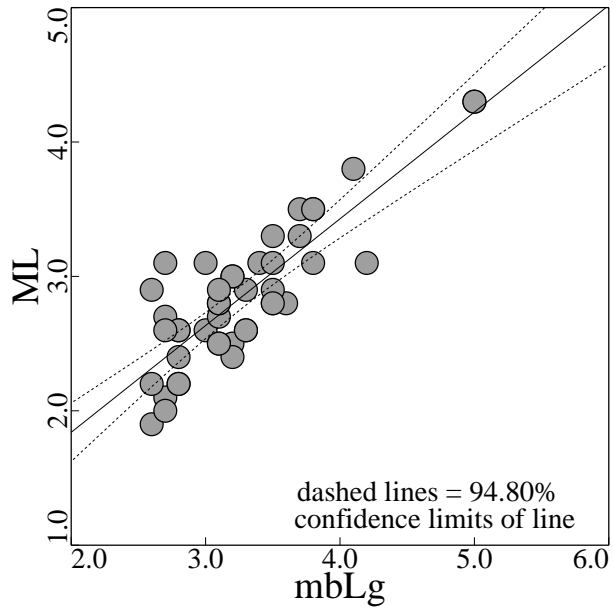
$$M_w = (1.165 \pm 0.175) \times m_{bL_g} - 1.191 \pm 0.088$$

(cor. coef.=0.953, std. error of est.=0.30, ndata=47)

Figure 12. M_w vs. m_{bL_g} scaling relationship for (a) $m_{bL_g} \leq 5.1$ and (b) $m_{bL_g} \geq 4.75$ earthquakes (events from Figure 11).

ML vs. mbLg: ENA

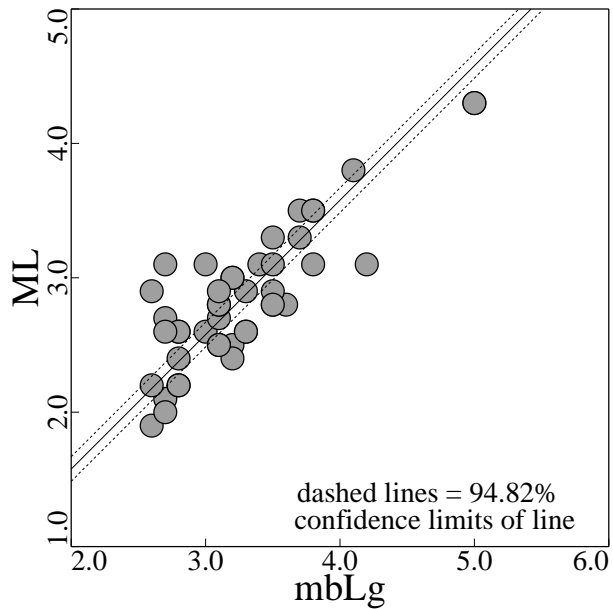
(a)



$ML = (0.794 \pm 0.153) \times mbLg + 0.252 \pm 0.085$
(cor. coef.=0.960, std. error of est.=0.28, ndata=44)

ML vs. mbLg: ENA

(b)



$ML = 1.000 \times mbLg - 0.423 \pm 0.091$
(cor. coef.=0.954, std. error of est.=0.30, ndata=44)

Figure 13. M_L vs. m_{bLg} scaling relationship for earthquakes in eastern North America: (a) unconstrained (free-slope) regression, (b) constrained (fixed-slope, $m = 1$) result. Event magnitudes taken from Ebel (1982).